ISSN 1023-9855

Thoracic Medicine

Volume 41 • Number 1 • March 2026

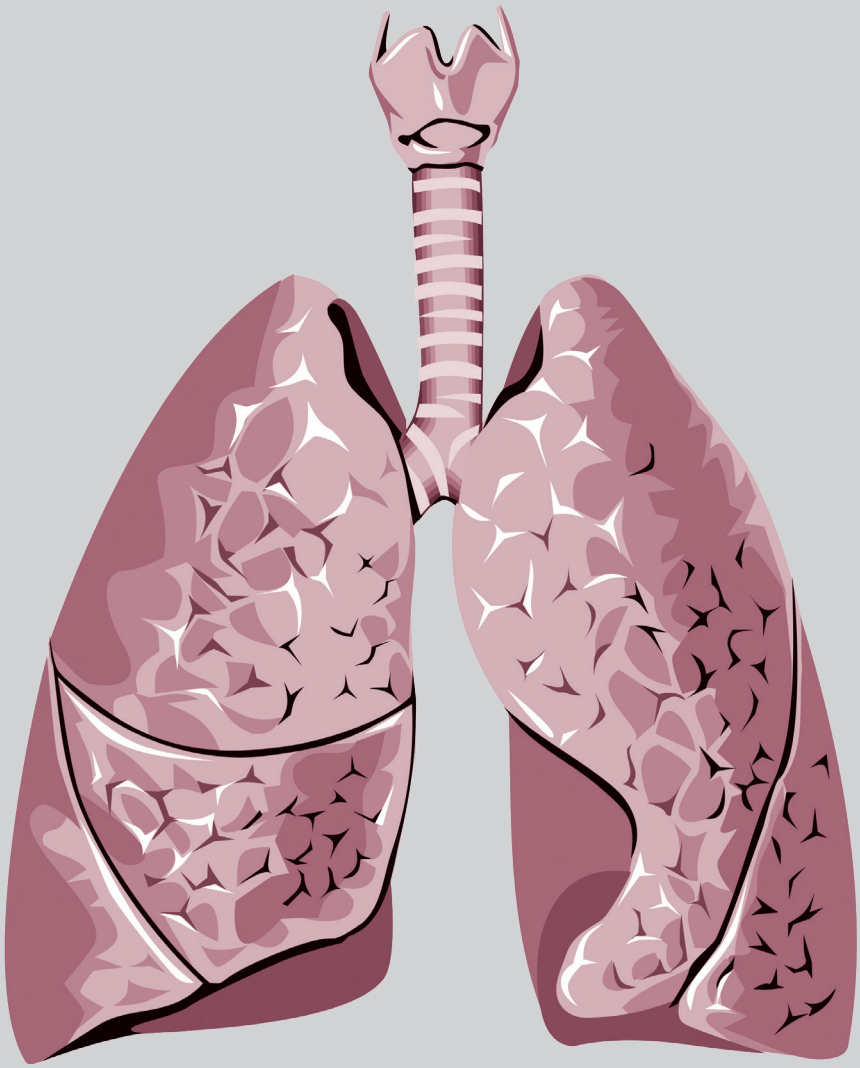

The Official Journal of

Taiwan Society of Pulmonary and Critical Care Medicine

Taiwan Society of Sleep Medicine

Taiwan Society for Respiratory Therapy

Taiwan Society of Tuberculosis and Lung Diseases

Thoracic Medicine

The Official Journal of
Taiwan Society of Pulmonary and Critical Care Medicine
Taiwan Society for Respiratory Therapy
Taiwan Society of Sleep Medicine
Taiwan Society of Tuberculosis and Lung Diseases

Thoracic Medicine

The Official Journal of
Taiwan Society of Pulmonary and Critical Care Medicine
Taiwan Society for Respiratory Therapy
Taiwan Society of Sleep Medicine
Taiwan Society of Tuberculosis and Lung Diseases

Volume 41
Number 1
March 2026

CONTENTS

Impact of Pulmonary Rehabilitation on COPD Patients

Chiao-Ning Hu[1*], Hsiu-Chin Wu[1*], Ya-Hui Wang[2], Yueh-Lan Huang[1], Cheng-Yi Wang[1], Ping-Keung Yip[3], Hen-I Lin[1]

Background: Chronic obstructive pulmonary disease (COPD) is a progressive lung condition that commonly presents with symptoms such as dyspnea, fatigue, reduced exercise capacity, and peripheral muscle dysfunction. These symptoms often lead to a diminished quality of life for patients. Pulmonary rehabilitation (PR) has been recognized as a therapeutic approach aimed at alleviating these clinical manifestations and improving patient outcomes. Despite its known benefits, there is limited research specifically addressing its impact on quality of life and lung function improvements in COPD patients. Therefore, this study aimed to evaluate the effectiveness of PR in enhancing both quality of life and lung function in patients with COPD.

Methods: This retrospective study analyzed data from patients enrolled in the national Pay-for-Performance (P4P) program for COPD at a teaching hospital between January 1, 2017 and December 31, 2020. Key parameters, including the Modified Medical Research Council scale, COPD Assessment Test, and lung function indicators such as FEV1 (L), FEV1 (%), and FEV1/FVC (%), were reassessed. Descriptive statistics were used to summarize patient characteristics, and inferential statistics were applied to assess the effects of PR.

Results: A total of 465 patients with COPD were included, with 298 in the control group and 167 in the PR group. Stratified analysis based on the occurrence of acute exacerbations in the preceding year revealed that PR improved mMRC scores. However, its effect on improving lung function parameters, including FEV1 (L), FEV1 (%), and FEV1/FVC (%), was not significant.

Conclusion: PR is effective in improving the mMRC scores of COPD patients, and in enhancing their quality of life. However, its impact on lung function parameters remains limited. ***(Thorac Med 2026; 41: 1-10)***

Key words: Chronic obstructive pulmonary disease, pulmonary rehabilitation

[1]Department of Internal Medicine, Cardinal Tien Hospital and School of Medicine, College of Medicine, Fu Jen Catholic University, New Taipei City, Taiwan. [2]Medical Research Center, Cardinal Tien Hospital and School of Medicine, College of Medicine, Fu Jen Catholic University, New Taipei City, Taiwan. [3]Division of Neurology, Cardinal Tien Hospital and School of Medicine, College of Medicine, Fu Jen Catholic University, New Taipei City, Taiwan.

*These authors contributed equally to this work.

Address reprint requests to: Dr. Yueh-Lan Huang, Department of Internal Medicine, Cardinal Tien Hospital and School of Medicine, College of Medicine, Fu Jen Catholic University, New Taipei City, Taiwan.

Introduction

Pulmonary rehabilitation (PR) has been increasingly recognized for its ability to improve physical endurance, making it a crucial component in the management of chronic obstructive pulmonary disease (COPD) [1]. Historically, COPD patients in Taiwan had limited access to PR. Recognizing the importance of PR, Taiwan's Ministry of Health and Welfare's National Health Insurance (NHI) Administration introduced the COPD Pay-for-Performance (P4P) improvement program on April 1, 2017 [2]. This initiative aims to elevate the standard of COPD care by integrating healthcare resources, promoting patient-centered care, enhancing patient monitoring and management, facilitating smoking cessation, offering health education services, and advocating for PR interventions. These measures seek to provide patients with comprehensive and continuous care, ultimately improving the quality of clinical treatment, reducing the frequency and severity of acute exacerbations, and diminishing readmission rates [3]. This concerted effort aims to establish a mutually beneficial scenario for patients, healthcare institutions, and the health department.

PR was endorsed through the COPD P4P program. Previous research has predominantly focused on strategies to shorten hospitalization durations, decrease acute exacerbation occurrences, lower mortality rates, or assess improvements in quality of life and walking distance following 3 months of PR [1]. However, few studies have explored enhancements in quality of life and lung function 1 year post-PR. Therefore, the present study sought to examine the impact of PR intervention on COPD patients.

Methods

The NHI COPD improvement program aims to reduce the burden of emergency room visits, ICU admissions, and COPD-related expenses. Hospitals/clinics participating in the P4P program may receive additional payments for case management, successful smoking cessation, implementation of PR, medication adherence, and reduction in COPD-related emergency visits and hospitalizations. The Taiwan COPD Clinical Practice Guidelines are used to establish uniform standards for physicians and to conduct evidence-based analyses of common COPD treatment methods [4]. Additionally, the Taiwan Society of Pulmonary and Critical Care Medicine organizes training and certification courses to enhance the skills and knowledge of physicians, case managers, and respiratory therapists. Patient decision aids and self-management tools are also provided by the Taiwan Society of Pulmonary and Critical Care Medicine.

Study Patients

The subjects in this study were patients who visited the chest outpatient department of a regional teaching hospital in New Taipei City from January 1, 2017 to December 31, 2020, and who were diagnosed with COPD and enrolled in the NHI COPD Improvement Program. The study aimed to assess the impact of PR on the disease after implementing the rehabilitation plan. We observed whether there were improvements in quality-of-life indicators and lung function indicators among the subjects who underwent PR and those who did not. Approval for this study was obtained from the Institutional Review Board (IRB) under the reference number CTH-110-3-5-050.

The subjects were divided into a PR group and a control group (non-PR group) based on whether they had visited the hospital's PR room

and underwent at least 1 PR procedure within 1 year after enrollment. The PR group consisted of 167 individuals, and the control group consisted of 298 individuals. The PR procedures included: negative pressure breathing assistance device, rehabilitation exercise, respiratory exercise (times), and steam or aerosol inhalation therapy each time. The lung function test and quality of life questionnaires, including the COPD Assessment Test (CAT) and Modified Medical Research Council (mMRC) were given.

Statistical Analysis

The data analysis for this study was conducted using IBM SPSS version 24.0 statistical software. The significance level (α level) was set at less than 0.05 for all statistical tests. For comparisons of pre- and post-test differences, paired t-tests and analysis of covariance (ANCOVA) were used. Additionally, simple and multiple linear regression was employed to investigate the association between undergoing PR and changes in the parameters of the quality of life questionnaires (mMRC, CAT) and lung function tests during the follow-up period.

Results

Baseline characteristics

This study examined the efficacy of PR in COPD patients enrolled in the COPD P4P improvement program at a regional teaching hospital in New Taipei City between 2017 and 2020. There were 465 participants.

Baseline demographics are outlined in Table 1 and show a comparable gender distribution between the PR (145 males, 22 females) and control groups (259 males, 39 females), with no significant difference ($p = 0.979$). The mean age was significantly higher in the PR group (71.75±9.92 years) than in the control group (69.49±10.59 years) ($p = 0.024$). Age stratification revealed significant differences between groups ($p = 0.039$).

Disease severity classification revealed significant disparities ($p < 0.001$) between the PR and control groups. The PR group predominantly fell into GOLD Groups B and D, while the control group had more individuals in Groups A and B. After adjustment based on the 2023 GOLD guidelines, Group E comprised 40.72% (PR) and 10.74% (control) of patients, with a significant difference ($p < 0.001$).

mMRC and CAT

Among cases without preceding-year severe acute exacerbation (SAE) before the index date, there were 255 individuals in the control group and 111 in the PR group (Table 2). The difference in mMRC scores from baseline (1.05±0.65) to 12 months (0.97±0.49) in the control group (p value of 0.711), and from baseline (1.48±0.83) to 12 months (1.24±0.55) in the PR group, with a *p*-value of 0.006, indicated a statistically significant improvement in the PR group compared to a minimal change in the control group. The CAT scores changed from baseline to 12 months in the control group and in the PR group, suggesting no significant difference between the groups but a tendency toward improvement with rehabilitation. Among cases with a preceding-year SAE before the index date, the difference in mMRC scores from baseline (1.23±0.68) to 12 months (1.08±0.48) in the control group (p value of 0.770), and from baseline (1.88±0.92) to 12 months (1.56±0.81) in the PR group, with a p-value of 0.002, indicated a statistically significant improvement in the PR group. CAT scores also showed no significant difference between groups, but a ten-

Table 1. Baseline Demographics (N=465).

	Control Group (N=298)		Pulmonary Rehabilitation Group (N=167)		*P* value
	n	(%)	n	(%)	
Enrollment years					0.119
2017	115	(38.59%)	67	(40.12%)	
2018	77	(25.84%)	52	(31.14%)	
2019	56	(18.79%)	33	(19.76%)	
2020	50	(16.78%)	15	(8.98%)	
Gender					0.979
Male	259	(86.91%)	145	(86.83%)	
Female	39	(13.09%)	22	(13.17%)	
Age (years), mean±SD	69.49±10.59		71.75±9.92		0.024
Age categories					0.039
40-59 years	48	(16.11%)	13	(7.78%)	
60-79 years	191	(64.09%)	118	(70.66%)	
>80 years	59	(19.8%)	36	(21.56%)	
GOLD Group					<0.001
A	125	(41.95%)	20	(11.98%)	
B	141	(47.32%)	79	(47.31%)	
C	8	(2.68%)	4	(2.4%)	
D	24	(8.05%)	64	(38.32%)	
GOLD Group (2023)					<0.001
A	125	(41.95%)	20	(11.98%)	
B	141	(47.32%)	79	(47.31%)	
E	32	(10.74%)	68	(40.72%)	
History of smoking					0.297
Never-smoker	56	(18.79%)	25	(14.97%)	
Smoking-related	242	(81.21%)	142	(85.03%)	
Comorbidity					
Myocardial infarction	5	(1.68%)	6	(3.59%)	0.214[a]
Congestive heart failure	13	(4.36%)	16	(9.58%)	0.026
Peripheral vascular disease	6	(20.1%)	0	(0%)	0.092[a]
Cerebrovascular disease	32	(10.74%)	13	(7.78%)	0.301
Peptic ulcer disease	43	(14.43%)	27	(16.17%)	0.615
Renal disease	17	(5.7%)	9	(5.39%)	0.087
Diabetes	37	(12.42%)	27	(16.17%)	0.260
Moderate or severe liver disease	20	(6.71%)	13	(7.78%)	0.666
Malignancy	13	(4.36%)	14	(8.38%)	0.075
BMI (kg/m^2), mean±SD	24.14±3.86		23.34±3.57		0.029

[a]Fisher's exact test.

GOLD: Global Initiative for Obstructive Lung Disease; BMI: body mass index

Table 2. Changes in mMRC, CAT and Pulmonary Function test Parameters During the Follow-up Period Between the Pulmonary Rehabilitation Group and the Control Group Stratified by Preceding-year Severe acute Exacerbation (SAE) Status.

Outcome measures	Control Group					Pulmonary Rehabilitation Group				
	Baseline		12 months		*P* value[a]	Baseline		12 months		*P* value[a]
	n	mean±SD	n	mean±SD		n	mean±SD	n	mean±SD	
Preceding year without SAE samples (n=366)										
mMRC score	255	1.05±0.65	156	0.97±0.49	0.711	111	1.48±0.83	84	1.24±0.55	0.006
CAT score	255	11.31±4.42	156	11.17±4.81	0.557	111	13.65±5.84	84	13.33±4.93	0.567
FEV1 (L)	255	1.76±0.59	149	1.79±0.6	0.838	111	1.49±0.52	80	1.56±0.64	0.290
FEV1 (%)	255	73.12±23.55	149	75.85±24.58	0.374	111	64.47±21.53	80	67.09±24.12	0.070
FEV1/FVC (%)	255	57.63±10.16	149	59.81±11.76	0.027	111	53.22±12.29	80	55.78±12.37	0.101
Post-bronchodilator test										
FEV1 (L)	255	1.85±0.59	145	1.88±0.61	0.311	111	1.58±0.53	77	1.66±0.68	0.302
FEV1 (%)	255	77.11±23.45	145	78.89±24.7	0.763	111	68.59±21.76	77	69.99±23.84	0.340
FEV1/FVC (%)	255	58.42±9.69	145	59.99±11.16	0.036	111	53.86±12.21	77	56.24±12.58	0.074
Preceding year with SAE samples (n=99)										
mMRC score	43	1.23±0.68	26	1.08±0.48	0.770	56	1.88±0.92	36	1.56±0.81	0.002
CAT score	43	11.26±4.97	26	11.54±4.85	0.406	56	15.70±6.18	36	13.94±6.42	0.055
FEV1 (L)	43	1.61±0.57	26	1.89±0.63	0.009	56	1.3±0.44	35	1.28±0.52	0.499
FEV1 (%)	43	66.19±20.22	26	77.58±21.25	0.006	56	55.55±19.61	35	56.17±24.23	0.447
FEV1/FVC (%)	43	55.79±10.2	26	60.16±11.59	0.019	56	49.73±13.43	35	49.4±14.2	0.328
Post-bronchodilator test										
FEV1 (L)	43	1.69±0.57	25	1.95±0.62	0.012	56	1.38±0.48	35	1.38±0.56	0.430
FEV1 (%)	43	69.72±21.02	25	80.68±21.62	0.008	56	58.7±20.46	35	57.57±26.83	0.904
FEV1/FVC (%)	43	55.84±10.02	25	61.2±11.88	0.002	56	50.09±12.5	35	50.46±14.19	0.135

[a]paired t test

mMRC :Modified Medical Research Council; *CAT : Chronic obstructive pulmonary disease* Assessment Test; FEV1: Forced expiratory volume in 1 second; FVC: Forced vital capacity

Table 3. Results of Analysis of Covariance (ANCOVA) with 12-month Outcome Measure as the Dependent Variable, Group as Fixed Effect, and Baseline Outcome Measure as Covariate Stratified by Preceding-year Severe Acute Exacerbation (SAE) Status.

Outcome measures	Difference in 12-month mean (pulmonary rehabilitation vs control; 95%CI)	*P* value
Preceding year without SAE samples (n=366)		
mMRC score	0.115 (-0.014, 0.244)	0.080
CAT score	1.236 (-0.036, 2.507)	0.057
FEV1 (L)	0.033 (-0.044, 0.109)	0.340
FEV1 (%)	0.291 (-3.297, 3.880)	0.873
FEV1/FVC (%)	-0.101 (-2.076, 1.875)	0.920
Post-bronchodilator test		
FEV1 (L)	0.064 (-0.021, 0.148)	0.138
FEV1 (%)	0.122 (-3.116, 3.359)	0.941
FEV1/FVC (%)	0.022 (-1.709, 1.752)	0.980
Preceding year with SAE samples (n=99)		
mMRC score	0.074 (-0.280, 0.428)	0.678
CAT score	0.878 (-2.383, 4.139)	0.592
FEV1 (L)	-0.237 (-0.440, -0.034)	0.023
FEV1 (%)	-11.360 (-19.539, -3.180)	0.007
FEV1/FVC (%)	-3.759 (-7.783, 0.266)	0.067
Post-bronchodilator test		
FEV1 (L)	-0.192 (-0.377, -0.007)	0.043
FEV1 (%)	-12.101 (-21.475, -2.728)	0.012
FEV1/FVC (%)	-4.506 (-8.627, -0.384)	0.033

mMRC : Modified Medical Research Council; CAT : Chronic obstructive pulmonary disease Assessment Test; FEV1: Forced expiratory volume in 1 second;FVC: Forced vital capacity.

dency toward improvement with rehabilitation. The differences in mMRC and CAT were not observed by ANCOVA (Table 3), regardless of whether the patients experienced SAE or not in the preceding year.

Lung function tests

The differences in lung function test results were also analyzed using paired t-tests (Table 2) and ANCOVA (Table 3). The difference in FEV1/FVC (%) from baseline to 12 months reached significance both before and after the bronchodilator test in the control group COPD patients without SAE in the preceding year. The differences in FEV1 (L), FEV1 (%), and FEV1/FVC (%) from baseline to 12 months reached significance both before and after the bronchodilator test in the control group COPD patients with SAE in the preceding year. In ANCOVA analysis, the differences between the control

and rehabilitation groups from baseline to 12 months showed significance in FEV1 (L) and FEV1 (%) before the bronchodilator test and in FEV1 (L), FEV1 (%), and FEV1/FVC (%) after the bronchodilator test.

Regression for mMRC, CAT and lung function

Simple linear regression showed a significant association between PR participation and mMRC changes (β = 0.124, p = 0.048) over 12 months, with baseline mMRC scores being a strong predictor (β = 0.359, p < 0.0001). In multiple regression, after adjusting for covariates, the effect of rehabilitation was no longer significant (β = 0.064, p = 0.310), but baseline mMRC (β = 0.312, p < 0.0001), age (β = 0.009, p = 0.002), and ICS use (β = 0.230, p = 0.046) remained significant (Table 4).

Simple regression showed a significant association between pulmonary rehabilitation and CAT score changes (β = 1.226, p = 0.041), with baseline CAT scores as a strong predictor (β = 0.348, p < 0.0001). In multiple regression, the effect of rehabilitation was non-significant (β = 0.666, p = 0.278), but baseline CAT scores (β = 0.313, p < 0.0001) and age (β = 0.084, p = 0.002) remained significant. SABA use was also significant (β = 1.538, p = 0.020) (Table 5).

Table 4. Simple and Multiple Linear Regression Models for mMRC Scores from Baseline During 12-month Follow-up of COPD Patients.

Variable	Simple linear regression			Mutiple linear regression		
	β	SE (*β*)	*p* value	*β*	SE (*β*)	*p* value
Intercept	0.626	0.053	<.0001	0.248	0.292	0.397
Rehabilitation group	0.124	0.062	0.048	0.064	0.063	0.310
Baseline mMRC score	0.359	0.038	<.0001	0.312	0.039	<.0001
SAE				-0.073	0.103	0.478
Age				0.009	0.003	0.002
Gender				-0.079	0.085	0.354
BMI				-0.008	0.007	0.288
CHF				0.178	0.116	0.125
Malignancy				-0.032	0.126	0.799
ICS				0.230	0.115	0.046
LABA+ICS				0.070	0.067	0.294
LABA+LAMA				-0.012	0.065	0.859
SABA				0.097	0.067	0.149
SAMA				0.120	0.109	0.271
Systemic beta agonist				-0.030	0.060	0.622

mMRC :Modified Medical Research Council;COPD: Chronic Obstruction Pulmonary Disease;SAE: Severe Acute Exacerbation; BMI: body mass index;CHF: Congestive heart failure;ICS: Inhaled corticosteroid; LABA: Long-acting beta2-agonist; LAMA: Long-acting muscarinic antagonists; SABA: Short-acting β2-agonist; SAMA: Short-acting muscarinic antagonists.

Table 5. Simple and Multiple Linear Regression Models for CAT Scores from Baseline During 12-month Follow-up of COPD Patients.

Variable	Simple linear regression			Mutiple linear regression		
	β	SE (β)	p value	β	SE (β)	p value
Intercept	7.430	0.687	<.0001	2.747	2.866	0.339
Rehabilitation group	1.226	0.598	0.041	0.666	0.614	0.278
Baseline CAT score	0.348	0.054	<.0001	0.313	0.055	<.0001
SAE				-0.820	0.998	0.412
Age				0.084	0.027	0.002
Gender				0.055	0.826	0.947
BMI				-0.063	0.073	0.384
CHF				-1.001	1.134	0.378
Malignancy				0.313	1.227	0.799
ICS				1.992	1.105	0.073
LABA+ICS				0.194	0.646	0.765
LABA+LAMA				0.548	0.630	0.385
SABA				1.538	0.658	0.020
SAMA				0.317	1.059	0.765
Systemic beta agonist				-0.174	0.581	0.765

CAT : Chronic obstructive pulmonary disease Assessment Test;COPD: Chronic Obstruction Pulmonary Disease;SAE: Severe Acute Exacerbation; BMI: body mass index;CHF: Congestive heart failure;ICS: Inhaled corticosteroid; LABA: Long-acting beta2-agonist; LAMA: Long-acting muscarinic antagonists; SABA: Short-acting β2-agonist; SAMA: Short-acting muscarinic antagonists.

Discussion

This study found significant results using the paired t-test, but not with ANCOVA, likely due to differences in baseline values between the PR and control groups. The paired t-test does not require identical baselines, making it suitable for this scenario, showing that PR significantly improves mMRC scores. However, ANCOVA assumes identical initial values, and the baseline differences violated this assumption, leading to non-significant results. Future randomized controlled trials with baseline-matched groups could provide more consistent findings.

Study results show that COPD patients who received PR showed a significant improvement in mMRC scores, reflecting changes in quality of life. In contrast, those who did not undergo rehabilitation either showed no change or a gradual deterioration. However, when examining lung function (e.g., FEV1 and FVC), no significant improvements were observed in either group, regardless of whether PR was provided. This indicates that while PR contributes to subjective quality of life, its effect on improving lung function appears limited. Additionally, lung function indices, such as FEV1 and FVC, showed a downward trend in both groups, suggesting that PR cannot effectively prevent pro-

gressive decline in lung function. Interestingly, the control group showed relatively more improvement in lung function, potentially due to selection bias, where patients with poor medication response and more severe symptoms were more likely to be included in the rehabilitation group, leaving the control group with relatively better baseline lung function.

Regarding mMRC, the results of simple and multiple linear regression analyses showed that baseline mMRC scores were the most significant factor influencing 12-month changes. Age and the use of ICS also significantly impacted mMRC scores. While PR initially showed an effect on improving mMRC in simple regression, this effect was no longer significant after adjusting for other variables, highlighting the dominant influence of baseline characteristics on mMRC changes. Baseline CAT scores and age were the primary factors influencing 12-month changes in COPD patients. The use of ICS and SABA also had a statistically significant impact on CAT scores. However, the effect of PR diminished in significance after adjusting for other variables, indicating that baseline characteristics and medication use played a more critical role in quality-of-life changes.

Although improvement in lung function was limited, the reason why PR can improve quality of life lies in the fact that engaging in PR can strengthen respiratory muscles, especially the diaphragm and intercostal muscles, making them more powerful and improving breathing during activity. Moreover, during exercise, breathing tends to adopt a deep and rapid pattern, which also develops respiratory muscle strength. Exercise also can increase the contractile ability of the heart muscle, helping to improve cardiovascular endurance and reduce the burden on the heart [5]. Furthermore, exercise training can strengthen the core muscle group and enhance overall coordination. A stable core muscle group helps to reduce the additional burden on respiratory muscles, making breathing easier, and thereby improving the subjective perception of quality of life in patients (mMRC and CAT) [6-7].

This study has several key strengths. First, it comprehensively records and analyzes quality of life questionnaires, including mMRC and CAT, from baseline to follow-up. This allows for a thorough understanding of changes in patient-reported outcomes as their conditions progress. Second, by incorporating lung function measurements, the study goes beyond subjective evaluations and investigates potential physiological changes, offering a more holistic view of the impact of PR. Third, the detailed records of patients' medication use and comorbidities enhance the reliability of the findings, as these factors are carefully considered and adjusted for in the statistical analysis. These strengths make the study more robust and comprehensive, providing valuable insights into the interplay between PR, quality of life, and lung function in COPD patients. The integration of detailed data on quality of life, lung function, and medication use ensures that the findings are both in-depth and relevant to clinical practice.

However, the study has notable limitations. First, its retrospective design and lack of randomization may introduce selection bias. For example, sicker patients were more likely to undergo PR, while healthier ones were not, as reflected in the higher prevalence of acute exacerbations in the rehabilitation group. Although statistical stratification methods were used to mitigate this bias, the absence of randomization remains a constraint. Second, the study is limited to a single regional teaching hospital

in New Taipei City. This restricts the ability to track acute exacerbation or treatments at other institutions, potentially underestimating the frequency of events. Broader data sources, such as the NHI database, could provide a more comprehensive view. Also, the study's follow-up period of 1 year may not capture the long-term effects of PR. Certain benefits or declines in lung function could require 2-3 years to fully manifest, limiting the scope of observed outcomes. Despite these challenges, the study still offers valuable contributions to understanding the role of PR in managing COPD.

Conclusion

Pulmonary rehabilitation showed improvements in mMRC, reflecting enhanced quality of life for COPD patients. However, in terms of lung function, including FEV1, FVC, and FEV1/FVC, whether before or after bronchodilator use, significant improvements were not consistently observed. These findings suggest that while PR effectively improves subjective outcomes, its impact on lung function may be limited.

Acknowledgments

This study was supported by grants from Cardinal Tien Hospital (CTH112A2217).

References

1. McCarthy B, Casey D, Devane D, *et al*. Pulmonary rehabilitation for chronic obstructive pulmonary disease. Cochrane Database Syst Rev 2015; 2015(2): CD003793.
2. Cheng SL, Li YR, Huang N, *et al*. Effectiveness of nationwide COPD pay-for-performance program on COPD exacerbations in Taiwan. Int J Chron Obstruct Pulmon Dis 2021; 18(16): 2869-81.
3. Agustí A, Celli BR, Criner GJ, *et al*. Global Initiative for Chronic Obstructive Lung Disease 2023 Report: GOLD Executive Summary. Eur Respir J 2023; 61(4): 2300239.
4. Cheng SL, Lin CH, Chu KA, *et al*. Update on guidelines for the treatment of COPD in Taiwan using evidence and GRADE system-based recommendations. J Formos Med Assoc 2021; 120(10): 1821-44.
5. Richardson CR, Franklin B, Moy ML, *et al*. Advances in rehabilitation for chronic diseases: improving health outcomes and function. BMJ 2019; 365: l2191.
6. Tout R, Tayara L, Halimi M. The effects of respiratory muscle training on improvement of the internal and external thoraco-pulmonary respiratory mechanism in COPD patients. Ann Phys Rehabil Med 2013; 56(3): 193-211.
7. Wouters EF, Posthuma R, Koopman M, *et al*. An update on pulmonary rehabilitation techniques for patients with chronic obstructive pulmonary disease. Expert Rev Respir Med 2020; 14(2): 149-61.

Outcome Predictors for Patients with Candidemia Receiving Prolonged Mechanical Ventilation

Yu-An Hsiao[1], Chen-Yiu Hung[1,2,3]

Background: Recently, candidemia has received considerable critical attention in intensive care units. Studies have shown the role of risk factor identification, molecular diagnosis, and new antifungal agents, although there have been mixed results and gaps in the early diagnosis.

Aim: To investigate the clinical characteristics, risk factors, and outcome predictors of candidemia in patients receiving prolonged mechanical ventilation (PMV).

Methods: Data of 45 candidemia patients receiving PMV between 2001 and 2012 were obtained. The patients' characteristics and outcomes were determined through a retrospective chart review, and data were evaluated using Student's t test, the chi-square test, and Fisher's exact test. Variables that were statistically significant ($p < 0.05$) in the univariate analysis were included in a multivariate analysis by multiple logistic regression. The variance inflation factor was used to identify any correlation between the independent variables and the strength of that correlation.

Results: Data from the survival and non-survival groups, comprising a total of 45 patients, were compared. The overall mortality rate was 71.1% (32/45). Both acute respiratory distress syndrome and steroid use may have had possible associations with candidemia, but the 2 variables were interconnected. The delay in starting antifungal treatment may have been associated with mortality.

Conclusion: Delay in starting appropriate antifungal treatment was associated with mortality. Additional prospective studies are required to identify these risk factors through a laboratory method to ensure timely treatment. ***(Thorac Med 2026; 41: 11-22)***

Key words: candidemia; acute respiratory distress syndrome; prolonged mechanical ventilation; sepsis; steroid

[1]Department of Thoracic Medicine, Chang Gung Memorial Hospital, Chang Gung University College of Medicine, Taoyuan, Taiwan. [2]Department of Respiratory Therapy, Chang Gung Memorial Hospital, Chang Gung University College of Medicine, Taoyuan, Taiwan. [3]Department of Respiratory Therapy, Chang Gung University College of Medicine.

Address reprint requests to: Dr. Chen-Yiu Hung, Department of Thoracic Medicine, Chang Gung Memorial Hospital, Taoyuan, Taiwan. 5 Fu-Hsin Street, Gweishan, Taoyuan, Taiwan, Zip 333.

Introduction

The incidence of invasive candidiasis, including bloodstream infection, has increased significantly in the last 10 years [1]. Candida species are the most common fungi causing nosocomial infections and are the fourth most common cause of nosocomial bloodstream infections in the United States [1-2]. The Candida infection candidemia increases the length of hospital stay, mortality rate, and health care cost [3-4]. Despite the advances in critical care and improvements in prophylactic antifungal agents, the mortality and morbidity of these patients remain major concerns.

To diagnose systemic fungal infections, positive culture from a normally sterile body fluid and histological evidence of tissue invasion are needed. In patients at a high risk of developing a Candida infection, a single positive test is only suggestive of such an infection, and it must be interpreted with caution because of false positive results caused by albumin, hemodialysis, or Gram-positive bacteremia [5]. The average Candida colonization index differed significantly between colonized and infected patients (0.47 and 0.70, respectively, $p < 0.01$) [6]. The 1,3-β-D-glucan test and antibodies against the mannan antigen were developed to detect the components of the fungal cell wall [7-8].

Given their nonspecific clinical features and the poor sensitivity of laboratory tests, the risk factors for invasive candidiasis have been evaluated using various scoring systems, including the Candida score, in surgical intensive care units (ICUs) [9]. Many studies on candidemia have also included medical ICU patients, and they have identified several risk factors, including old age and septic shock. However, only a few studies have focused on patients with candidemia requiring prolonged mechanical ventilation (PMV), who typically have severe illnesses that preclude the discontinuation of ventilator use. Therefore, the current study aimed to investigate the clinical characteristics, risk factors, and outcome predictors of candidemia in patients receiving PMV.

Material and Methods

Patient information and data collection

A total of 2079 patients with candidemia diagnosed based on direct fungal detection in blood cultures, who were admitted at Linkou Chang Gung Memorial Hospital (Taipei, Taiwan) between January 2001 and December 2012, were enrolled. Only the data on the first admission episode was analyzed for patients with more than 1 ICU admission during the study period. The exclusion criteria were as follows: patients aged <18 years, those who had received mechanical ventilation (MV) for <21 days, and who had developed candidemia within the first 21 days of MV, or had solid organ or hematopoietic stem cell transplantation, chemotherapy, or immunosuppressant treatment within 7 days before ICU admission. No patient received selective decontamination of the digestive tract or antifungal prophylaxis in our ICU during the study period.

The primary criterion for selecting patients was having received PMV (for >21 days) followed by transfer to the respiratory care center (RCC). The RCC is a 24-bed ICU within the 3800-bed tertiary medical center of Linkou Chang Gung Memorial Hospital. This RCC facility has nurse-to-patient and respiratory therapist-to-patient ratios of 1:3 and 1:8, respectively. The RCC unit was established as part of

a policy transferring responsibility for ICU patients experiencing weaning difficulty [10]. Patients had been maintained on MV for >3 weeks and all previous weaning attempts had failed. Patients were eligible for RCC admission if they met the following conditions: hemodynamic stability without vasoactive drug treatment, stable oxygen requirements (fraction of inspired oxygen ≥40%, positive end expiratory pressure <10 cm H_2O, and peak inspiratory pressure <35 cm H_2O), no acute hepatic or renal failure, and no requirement for surgical intervention within the ensuing 2 weeks. Any patient who became hemodynamically unstable or had multiple organ failure was transferred back to the appropriate ICU. Primary care was provided by intensivists. Patients admitted to the RCC received customized levels of respiratory rehabilitation, depending on their consciousness level and limb movement limitation [10]. Linkou Chang Gung Memorial Hospital and Chang Gung Medical Foundation (IRB no. 103-1251B) approved our study protocol. This work was supported by grants CMRPG3D1213, CMRPG3J1771, CMRPG3J1501, CMRPG3L1671, CMRPG3J1501, CMRPVVJ 0052 from Chang Gung Memorial Hospital.

Data were collected retrospectively by reviewing the patients' medical records from January 1, 2001 to December 31, 2012. On the first day of ICU admission, we recorded the patients' age, sex, underlying diseases, date and cause of respiratory failure, MV settings (days 1 and 21), laboratory analyses, hemodynamic status, renal and hepatic functions, and corticosteroid use. The acute physiology and chronic health evaluation (APACHE) II and sequential organ failure assessment scores were calculated for each respiratory patient within the first 24 hours and on the day of RCC admission (MV day 21). The outcome variables were the following: discharge status, MV duration, lengths of hospital and RCC stays, and cause of death.

Definitions

The death of a patient with PMV, irrespective of the duration or cause of the respiratory failure, from any cause related to or aggravated by candidemia or its management, is defined. Actual death times (in days) were recorded for correct censoring at 30 days. Acute respiratory distress syndrome (ARDS) was defined using the Berlin definition and classified as mild, moderate, or severe [11]. Sepsis-related ARDS was defined as ARDS that developed in patients with sepsis, whereas non-sepsis-related ARDS was defined as ARDS that developed after non-septic injuries, such as trauma, aspiration, and multiple transfusions [12]. A major operation was defined as a surgical procedure involving the intrathoracic, intraabdominal, cardiac, or intracranial area. Shock was defined as a mean arterial pressure <65 mmHg accompanied by evidence of hypoperfusion or a vasopressor support requirement. The presence of septic shock was recorded during the episode of sepsis, at which, blood cultures samples, which tested positive for candidemia, were collected. Colonization was defined as the presence of Candida spp. in 3 or more samples obtained from the same or different body sites on at least 2 consecutive screening days [5]. Corticosteroid use was defined as ≥0.3 mg/kg/day of prednisolone-equivalent corticosteroids for at least 14 days, based on the body weight-adjusted dose distribution in our cohort (mean body weight: 60.8 ± 10.2 kg). Candidemia was diagnosed if Candida species were isolated from the patients' blood cultures within 1 week of invasive fungal infection (IFI)

diagnosis.

Microbiological examination

Blood cultures were performed on patients having systemic inflammatory response syndrome with a suspected infection. Automated blood culture systems were used in our microbiology laboratory. Isolates were identified using standard phenotypic techniques. Catheter tips were processed using a semiquantitative culture method, and blood cultures were examined based on routine methods using a semi-automatic culture detector. Central venous catheter (CVC) colonization was defined as the absence of positive blood culture drawn through an intravenous line and a positive semiquantitative catheter tip culture without any clinical infection symptom or sign [6].

Statistical analysis

Data were analyzed with SPSS 22.0 (SPSS Inc., Chicago, IL, USA). The characteristics of the survival and non-survival groups were compared using the chi-squared test for categorical variables and the independent t-test for continuous variables. If the cells of a 2 × 2 table had an expected count of <5, Fisher's exact test was used. All statistical tests were 2-tailed, and a p value of <0.05 was considered statistically significant. The risk factors for IFI were initially assessed by univariate analysis. Variables that were statistically significant ($p < 0.05$) in the univariate analysis were included in a multivariate analysis by multiple logistic regression based on the backward elimination of data. The variance inflation factor (VIF) was used to identify a correlation between independent variables and the strength of that correlation. This index offers a metric to gauge variance increases (squared value of the estimate's standard deviation) of a predicted regression coefficient due to collinearity.

Results

Blood cultures were processed according to routine methods using a semi-automatic culture detector. Altogether, 2079 patients tested positive for blood fungus with a Candida infection at our institution from January 1, 2001 to December 31, 2012, and 1240 of these patients experienced respiratory failure requiring MV. We excluded 37 patients due to young age, 17 due to a history of solid organ (n = 7) or hematopoietic stem cell (n = 10) transplantation, and 13 due to chemotherapy or immunosuppressant use before the IFI diagnosis. Of these 1240 patients, 45 had intubation with MV for >21 days and were enrolled in our study (Fig. 1).

Table 1 presents a comparison of the general characteristics and underlying conditions of the survival (n = 13) and non-survival (n = 32) groups. The overall mortality rate was 71.1% (32/45). The APACHE II scores on days 1 and 21 did not differ (22.4 vs. 22.3, $p = 0.94$; and 18.4 vs.18.5, $p = 0.87$, respectively). The non-survival group exhibited a higher incidence of end-stage renal disease with hemodialysis (38.5% vs. 46.8%, $p = 0.75$), hepatobiliary disease (0 vs. 9.4%, $p = 0.55$), solid tumor (7.6% vs. 34.3%, $p = 0.13$), and hematologic malignancy (7.6% vs. 21.9%, $p = 0.40$); however, these differences were not statistically significant.

Table 2A presents the patient factors related to PMV. Before the occurrence of an IFI, ARDS occurred in 7.6% and 53.1% of the survival and non-survival groups, respectively ($p = 0.01$). In the non-survival group, sepsis-related ARDS constituted 80% of the ARDS (12 patients),

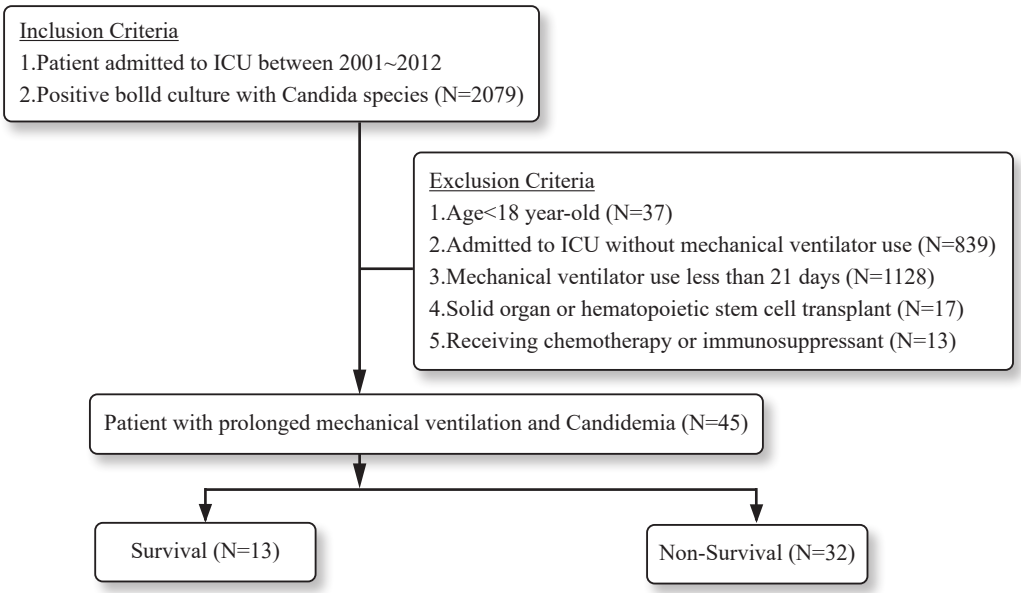

Fig. 1. Schematic of analysis of ICU patients with candidemia receiving prolonged mechanical ventilation. ICU = intensive care unit.

Table 1. Comparison of the Characteristics of the Surviving and non-Surviving Patients with Invasive Candidiasis Receiving Prolonged Mechanical Ventilation.

	Survival (N = 13)	Non-survival (N = 32)	*p* value
General Characteristics			
Age	70.7 ± 15.6	74.8 ± 12.8	0.17
Male gender	13 (46%)	26 (58%)	0.35
APACHE II (ICU Day 1)	22.4 ± 7.3	22.3 ± 6.9	0.94
APACHE II (Day 21)	18.4 ± 4.9	18.5 ± 4.7	0.87
Overall ventilation hours	840 ± 10.2	775.7 ± 11.1	0.48
Median day of candidemia detection	35 ± 10.2	32.3 ± 11.1	0.57
Underlying Disease			
Chronic kidney disease	6 (46.1%)	20 (62.5%)	0.34
ESRD with hemodialysis	5 (38.5%)	15 (46.8%)	0.75
Hepatobiliary disease	0 (0%)	3 (9.4%)	0.55
Asthma	2 (15.4%)	5 (15.6%)	1.00
COPD	3 (23.1%)	6 (18.8%)	0.70
Tuberculosis	2 (15.4%)	5 (15.6%)	0.99
Cerebrovascular disease	10 (76.9%)	14 (43.8%)	0.05
Heart failure	7 (53.8%)	13 (40.6%)	0.51
Underlying solid tumor	1 (7.6%)	11 (34.3%)	0.13
Underlying hematologic malignancy	1 (7.6%)	7 (21.9%)	0.40
Chronic kidney disease	6 (46.1%)	20 (62.5%)	0.34

*P-value <0.05

+ Data represent the mean ± S.D or the number of patients with the ratio in parentheses.

APACHE: Acute Physiology and Chronic Health Evaluation; ICU: intensive care unit; COPD: chronic obstructive pulmonary disease

Table 2A. Risk Factor Analysis of Invasive Candidiasis Patients with Prolonged Mechanical Ventilation (Pearson's chi-squared test with Fisher's exact analysis).

	Survival (N = 13)	**Non-survival (N = 32)**	***p* value**
Cause of Prolonged Mechanical Ventilation			
ARDS	1 (7.6%)	17 (53.1%)	0.01*
Sepsis-related ARDS	0	12 (37.5%)	0.01*
Non-sepsis-related ARDS	1 (7.7%)	5 (15.6%)	0.81
Multiple organ failure	10 (76.9%)	17 (53.1%)	0.18
Cardiac disease	3 (23.1%)	18 (56.3%)	0.06
Major operation	6 (46.1%)	7 (21.9%)	0.15
Neuromuscular disease	6 (46.1%)	6 (18.8%)	0.08
Candidemia Predisposing Factor			
Febrile neutropenia	2 (15.3%)	4 (12.5%)	1
Major operation	3 (23.1%)	7 (21.9%)	1
Tracheostomy	9 (69.2%)	20 (62.5%)	0.74
Total parenteral nutrition	2 (15.3%)	5 (15.6%)	0.99
Candida colonization index	0.51 ± 0.08	0.53 ± 0.10	0.18
Central venous catheter use	11 (84.6%)	20 (62.5%)	0.25
Site of positive culture result			
Central venous catheter	12 (92.3%)	20 (62.5%)	0.07
Urine fungus culture	10 (76.9%)	4 (12.5%)	0.01*
Sputum fungus culture	1 (7.6%)	6 (18.8%)	0.32
Ascites culture	0	0	0
Septic shock	10 (76.9%)	23 (71.9%)	1
Appropriate antifungal agent use within 48 hours	10 (76.9%)	10 (31.6%)	0.01*
Acute respiratory distress syndrome	1 (7.6%)	17 (53.1%)	0.01*
High-dose steroid use (>20 mg × 14 days)	2 (15.3%)	18 (56.3%)	0.02*
Steroid use duration (days)	14.2 ± 0.6	16.5 ± 3.4	0.03*
Accumulative steroid dose (mg)	618.3 ± 247.1	818.9 ± 308.1	0.04*

**P*-value <0.05

+ Data represent the mean ± S.D. or the number of patients with the ratio in parentheses.

† Appropriate antifungal therapy was defined as: fungal species susceptible, corrected daily dose, and time-to-initiation within 48 hrs of detection of candidemia.

ARDS: acute respiratory distress syndrome CVC: central venous catheter

trauma (3 patients), and pneumonia (2 patients) cases. One patient with candidemia and sepsis-related ARDS due to aspiration pneumonia survived. The ARDS patients in the non-survival group had either moderate (n = 13) or severe ARDS (n = 4), according to the Berlin definition. The surviving patient with ARDS (n = 1) was considered to have had mild ARDS.

Table 2A also presents the possible predisposing factors of candidemia. The results indi-

cated that the use of high-dose corticosteroids (prednisolone ≥20 mg for at least 14 days) was significantly associated with poor patient outcomes. We noted a relationship among the outcomes of the Candida colonization index, but the differences were not statistically significant between the survival and non-survival groups (0.51 vs. 0.53, p= 0.18). The survival group exhibited a higher incidence of urine colonization (83.3% vs. 14.3%, p = 0.03), whereas the non-survival group exhibited a higher incidence of sputum colonization (8.3% vs. 21.4%, p = 0.23); however, the differences were not statistically significant. Ten patients (22.2%) had a major operation before transfer to the RCC; 3 of these patients (6.6%) underwent abdominal surgery with TPN use, and 5 (11%) received TPN due to malnutrition.

Among those receiving the appropriate antifungal agents, the mean duration from onset of sepsis to the administration of the appropriate antifungal (or mean delay of antifungal therapy) was 2.72 days (0–5 days). The risk factors identified by univariate analysis were ARDS (N = 1, 7.6% vs. N = 17, 53.1%, p = 0.01), steroid use duration (14.2 vs. 16.5 days, p = 0.03), accumulative steroid dosage (618.3 vs. 818.9 mg, p = 0.04), and antifungal agent use within 48 hours (N = 10, 76.9% vs. N = 10, 31.6%, p = 0.01). Table 2B shows the results of our multivariate

Table 2B. Univariate and Multivariate Analyses of Clinical Variables Associated with Mortality in Candidemia Patients.

	Univariate analysis			Multivariate analysis		
Variables	**Odds ratio**	**95% C.I.**	***p* value**	**Odds ratio**	**95% C.I.**	***p* value**
Febrile neutropenia	0.24	0.20–76.68	0.54			
Major operation	0.604	0.02–19.86	0.78			
Tracheostomy	55626.86	0	0.99			
Total parenteral nutrition	1.594	0.01–529.56	0.88			
Central venous catheter use	0	0	1.00			
Candida colonization index	0.08	−1.221–1.944	0.65			
Site of positive culture result						
Central venous catheter	0	0	1.00			
Urine fungus culture	0.96	0.012–77.07	0.98			
Sputum fungus culture	3.08	0.01–984.65	0.70			
Septic shock	131655	0	0.99			
Antifungal agent use within 48 hrs	0.022	0.001–0.361	0.02*	0.14	0.02–0.832	0.03*
Acute respiratory distress syndrome	17.86	3.47–9641.49	0.04*	13.34	0.31–579.82	0.18
High dose steroid use	3.77	0.01–4.806	0.04*	5.83	0.02–15.66	0.75
Steroid use duration (days)	2.28	1.59–18.07	0.03*	8.43	1.83–37.245	0.99
Accumulative steroid dose (mg)	1.3	1.01–1.81	0.04*	9.04	0.01–12.87	0.99

**P*-value <0.05

+ Data represent the mean ± S.D or the number of patients with the ratio in parentheses.

CVC: central venous catheter

analysis of the variables associated with IFIs. The results indicate that antifungal agent use within 48 hours was significantly and independently associated with IFIs.

To isolate the relationship between each independent variable and the dependent variable, the impact of the existence of multicollinearity among the predictor variables on the hypotheses testing decision taken can be seen in Table 3. These results show that the time-to-antifungal agent use was statistically significant. Time-to-antifungal agent use has a VIF near 1, showing that it is not affected by multicollinearity. We have included the interaction term of ARDS * steroid dosage and ARDS * steroid usage duration. The VIFs indicate that ARDS and steroid use may have severe multicollinearity for both the main effect and interaction term.

Fig. 2 depicts the distribution of different Candida species. The major species in the order

Table 3. Multicollinearity in regression analysis: outcome versus ARDS, steroid, funguria, and antifungal agent use.

Term	Coef	SE Coef	T value	*P* value	VIF
Constant	0.832	0.131	6.369	0	
ARDS	0.467	1.31	1.505	0.141	5.814
Accumulative steroid dosage (mg)	−0.146	1.297	−0.49	0.627	5.503
Duration of steroid use (days)	0.361	0.782	0.462	0.647	3.311
Funguria	−0.218	0.145	−1.501	0.142	1.203
Time to antifungal agent use (hours)	−0.372	0.138	−2.694	0.011	1.198
ARDS * steroid (mg)	−0.008	0.001	−0.095	0.049	9.971
ARDS * steroid (days)	0.024	0.383	0.812	0.422	9.336

When correlation exists among the predictors, the standard error of predictor coefficients will increase, and the variance of predictor coefficients is inflated. The VIF is considered highly correlated if VIF >5. Coef: correlation coefficients; SE Coef: standard error of coefficients; VIF: variance inflation factor; ARDS: acute respiratory distress syndrome.

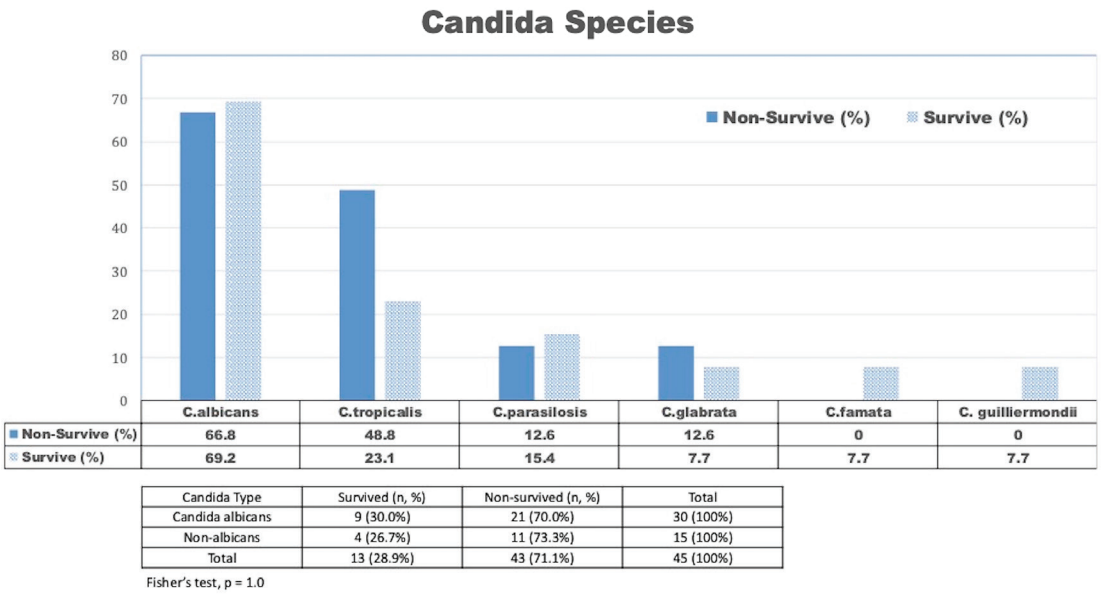

Fig. 2. Comparison of infecting *Candida* species between the survival and non-survival groups. A Fisher's exact test comparing mortality between *Candida albicans* and non-*albicans Candida* showed no significant difference ($p = 1.0$). ICU = intensive care unit.

of decreasing frequency were as follows: Candida albicans (survivors: 69.2% vs. non-survivors: 66.8%), C. tropicalis (survivors: 23.1% vs. non-survivors: 48.8%), C. parasilosis (survivors: 15.4% vs. non-survivors: 12.6%), and C. glabrata (survivors: 7.7% vs. non-survivors: 12.6%). C. fumata and C. guilliermondii had a single case each. In addition, we performed a Fisher's exact test comparing mortality between patients with Candida albicans and those with non-albicans Candida infections. The results showed no statistically significant difference (p = 1.000). Most of the patients had only one Candida species in the blood culture sample; however, the samples from 4 non-survivors had 2 Candida species (C. albicans and C. glabrata) during the index episode of sepsis.

Discussion

Invasive candidiasis has been reported to be responsible for a large proportion of cases of mortality and morbidity among patients with nosocomial infections. Both ARDS and steroid use may have possible associations with the development of invasive candidiasis, but the 2 variables were interconnected due to the common use of steroids for the treatment of ARDS in the study patients. It is possible that the delay in starting antifungal treatment was associated with mortality.

The average incidence of Candida bloodstream infections in an ICU was reported to be 7.4 per 10,000 patient days, and the overall mortality rate of patients with candidemia was 58% [13-14]. In our hospital, 18% of patients with hematologic malignancy receiving transplantation were transferred to the ICU and provided with MV; furthermore, 33% of these patients had IFI [15]. The mortality rate was 85% among these patients [15]. In the current study, we found a mortality rate of up to 70% in patients receiving PMV, which is higher than that in the general ICU population and lower than that among patients receiving transplants and admitted to the ICU. Although C. albicans remains the most frequent species isolated in candidemia in ICU patients, an increased proportion of non-albicans Candida spp., in particular C. glabrata, has been reported [16]. Given the limited sample size, we compared mortality between Candida albicans and non-albicans Candida and found no significant difference (Fisher's test, p = 1.0). Chi HW, *et al*. have reported high all-cause mortality in patients with C. albicans and in those with non-albicans spp. [17]. Candidemia, independent risk factors, and local epidemiology need further study to differentiate fatal candidemia from non-fatal candidemia.

CVC use, prolonged systemic antibiotics use, total parenteral nutrition, hemodialysis, major surgery, systemic steroids, systemic immunosuppressive agent use at 7 days prior to ICU admission, or neutropenia may increase the incidence of IFI [14, 18]. In the current study, the use of high-dose corticosteroid (≥20 mg of prednisolone for at least 14 days) was significantly associated with poor patient outcomes. Two patients from the survival group received 30 mg of prednisolone per day for chronic obstructive pulmonary disease (COPD). Among the 18 non-survivors, 14 received corticosteroids for ARDS (40 mg of methylprednisolone every 12 hours for >10 days) and 4 received an equivalent dose for COPD acute exacerbation. Additional studies are necessary to clarify the relationship between accumulative steroid dosage and IFI [19-21]. The purpose of steroid therapy, thresholds of steroid therapy, and exact

safety margin of steroid use have not been thoroughly evaluated.

When comparing the survival group to the non-survival group among candidemia patients in our study, ARDS and steroid use may have had severe multicollinearity for both the main effect and the interaction period. Glucocorticoids may improve oxygenation and hasten radiographic improvement in ARDS patients, but these agents have no consistent survival benefit and are harmful if started at >14 days after ARDS diagnosis [22]. Defective T-cell immunity contributes both to the development of ARDS and a disseminated Candida infection, and the inability to control candidemia also contributes to the increased mortality [23-24]. From a clinical point of view, 2 possible factors may explain this result. First, we determined that sepsis-related ARDS is the major etiology of ARDS in our study. Sepsis alone is an independent risk factor for IFI [25]. Second, 14 out of 17 patients with ARDS (82.3%) received high-dose corticosteroids for ARDS. The finding that ARDS increased the mortality rate might only serve to confirm that ARDS was indeed related to poor patient outcomes.

Early diagnosis and adequate treatment are critical to achieving a favorable outcome. Blood cultures remain the major diagnostic method, but suboptimal sensitivity (30%–50%) and the long incubation time required may delay treatment [26]. Kao *et al*. reported the role of open lung biopsy in selected patients with ARDS in our center; pathological findings of infectious disease in ARDS patients were found to be associated with hospital mortality [27]. Given the time-consuming laboratory methods and importance of proper antifungal drug therapy, several researchers have suggested a Candida score [5]. Fungus culture remains the gold standard for making a diagnosis, but simple colonization is always difficult to distinguish from active infections. The existence of true Candida pneumonia is doubtful and recovery of Candida spp. from the respiratory tract using bronchoalveolar lavage might be considered as colonization and could not justify antifungal therapy [28-29]. Measuring the serum or plasma beta-D-glucan and gallactoman (BDG) has a high level of accuracy in determining patients with and without IFIs, mainly IFIs due to Candida or Aspergillus [26, 30]. The identification of these risk factors for ensuring timely treatment before laboratory evidence of infection is essential in the ICU.

Our study had 5 major limitations. First, we categorized the patients diagnosed with invasive candidiasis into the survival and non-survival groups. Neither observation holds much validity because the number of patients was extremely low and the causes of mortality were not verified. In addition, although a more detailed comparison of mortality across all Candida species would be informative, the limited sample size constrains the statistical reliability of such an analysis. Second, our study was retrospective and performed at a single center; therefore, the findings have limited generalizability. Third, the previous use of antifungal agents, such as azoles and echinocandins, and the duration of medication prescription may lead to different results. Different antifungal agents may lead to different treatment efficacies with the same Candida spp., suggesting the antifungals could be a variable for the analysis of factors associated with mortality. Fourth, multicollinearity is a serious problem before starting the data modeling process. Combining the highly correlated variables through a principal component analysis or omitting a variable from the analysis that is associated with other variables is highly

needed in future studies. Fifth, BDG has been included in the relevant diagnostic criteria of the European Organization for Research and Treatment of Cancer/Mycoses Study Group, but BDG data were not available for this study before 2014, requiring further prospective studies to clarify.

Conclusion

In our study, both ARDS and steroid use may have had possible associations with candidemia, and the 2 variables were interconnected due to the common use of steroids in the study patients for the treatment of ARDS. A potential association between delayed initiation of antifungal treatment and mortality warrants further investigation. Additional prospective studies are required to identify the risk factors through a laboratory method to ensure timely treatment.

Compliance with Ethical Standards.

Acknowledgments

Linkou Chang Gung Memorial Hospital and Chang Gung Medical Foundation (IRB no. 103-1251B) approved our study protocol. This work was supported by grants CMRPG3D1213, CMRPG3J1771, CMRPG3J1501, CMRPG3L1671, CMRPG3J1501, and CMRPVVJ 0052 from Chang Gung Memorial Hospital.

References

1. Nawaf A, Sameera A, Laila L, *et al*. Candida bloodstream infection: changing pattern of occurrence and antifungal susceptibility over 10 years in a tertiary care Saudi hospital. Can J Infect Dis Med Microbiol 2019; 2015692.
2. Chen PY, Chuang YC, Wang JT, *et al*. Comparison of epidemiology and treatment outcome of patients with candidemia at a teaching hospital in Northern Taiwan, in 2002 and 2010. J Microbiol Immunol Infect 2014; 47: 95-103.
3. Darouiche RO. Candida in the ICU. Clin Chest Med 2009; 30:287-93, vi-vii.
4. Blot S, Dimopoulos G, Rello J, *et al*. Is Candida really a threat in the ICU? Curr Opin Crit Care 2008; 14: 600-604.
5. Eggimann P, Pittet D. Candida colonization index and subsequent infection in critically ill surgical patients: 20 years later. Intensive Care Med 2014; 40:1429-1448.
6. Pittet D, Monod M, Suter PM, *et al*. Candida colonization and subsequent infections in critically ill surgical patients. Ann Surg 1994; 220: 751-758.
7. Ahmad S, Khan Z. Invasive candidiasis: a review of nonculture-based laboratory diagnostic methods. Indian J Med Microbiol 2012; 30: 264-269.
8. Peman J, Zaragoza R. Current diagnostic approaches to invasive candidiasis in critical care settings. Mycoses 2010; 53: 424-433.
9. Leon C, Ruiz-Santana S, Saavedra P, *et al*. A bedside scoring system ('Candida score') for early antifungal treatment in nonneutropenic critically ill patients with Candida colonization. Crit Care Med 2006; 34: 730-737.
10. Wu YK, Tsai YH, Lan CC, *et al*. Prolonged mechanical ventilation in a respiratory-care setting: a comparison of outcome between tracheostomized and translaryngeal intubated patients. Crit Care 2010; 14: R26.
11. ARDS Definition Task Force, Ranieri VM, Rubenfeld GD, *et al*. Acute respiratory distress syndrome: the Berlin Definition. JAMA 2012; 307: 2526-2533.
12. Sheu CC, Gong MN, Zhai R, *et al*. Clinical characteristics and outcomes of sepsis-related vs non-sepsis-related ARDS. Chest 2010; 138: 559-567.
13. Gonzalez de Molina FJ, Leon C, Ruiz-Santana S, *et al*. Assessment of candidemia-attributable mortality in critically ill patients using propensity score matching analysis. Crit Care 2012; 16: R105.
14. Cornely OA, Bassetti M, Calandra T, *et al*. ESCMID guideline for the diagnosis and management of Candida diseases 2012: non-neutropenic adult patients. Clin Microbiol Infect 2012; 18: 19-37.
15. Hung CY, Kao KC, Wang PN, *et al*. Invasive fungal infection among hematopoietic stem cell transplantation patients with mechanical ventilation in the intensive care

unit. BMC Infect Dis 2012; 12: 44.
16. Lamoth F, Lockhart SR, Berkow EL, *et al*. Changes in the epidemiological landscape of invasive candidiasis. J Antimicrob Chemother 2018; 73: i4-i13.
17. Chi HW, Yang YS, Shang ST, *et al*. Candida albicans versus non-albicans bloodstream infections: the comparison of risk factors and outcome. J Microbiol Immunol Infect 2011; 44: 369-375.
18. Pappas PG, Kauffman CA, Andes D, *et al*. Clinical practice guidelines for the management of candidiasis: 2009 update by the Infectious Diseases Society of America. Clin Infect Dis 2009; 48: 503-535.
19. Lionakis MS, Kontoyiannis DP. Glucocorticoids and invasive fungal infections. Lancet 2003; 362: 1828-1838.
20. Zilberberg MD, Kollef MH, Arnold H, *et al*. Inappropriate empiric antifungal therapy for candidemia in the ICU and hospital resource utilization: a retrospective cohort study. BMC Infect Dis 2010; 10: 150.
21. Han SS, Yim JJ, Yoo CG, *et al*. Clinical characteristics and risk factors for nosocomial candidemia in medical intensive care units: experience in a single hospital in Korea for 6.6 years. J Korean Med Sci 2010; 25: 671-676.
22. Steinberg KP, Hudson LD, Goodman RB, *et al*. Efficacy and safety of corticosteroids for persistent acute respiratory distress syndrome. N Engl J Med 2006; 354: 1671-1684.
23. Romani L. Immunity to fungal infections. Nat Rev Immunol 2011; 11: 275-288.
24. Miceli MH, Diaz JA, Lee SA. Emerging opportunistic yeast infections. Lancet Infect Dis 2011; 11: 142-151.
25. Gonzalez de Molina FJ, Leon C, Ruiz-Santana S, *et al*. Assessment of candidemia-attributable mortality in critically ill patients using propensity score matching analysis. Crit Care 2012; 16: R105.
26. Mikulska M, Calandra T, Sanguinetti M, *et al*. The use of mannan antigen and anti-mannan antibodies in the diagnosis of invasive candidiasis: recommendations from the Third European Conference on Infections in Leukemia. Crit Care 2010; 14: R222.
27. Kao KC, Hu HC, Chang CH, *et al*. Diffuse alveolar damage associated mortality in selected acute respiratory distress syndrome patients with open lung biopsy. Crit Care 2015; 19: 228.
28. Rose SR, Vallabhajosyula S, Velez MG, *et al*. The utility of bronchoalveolar lavage beta-D-glucan testing for the diagnosis of invasive fungal infections. J Infect 2014; 69: 278-283.
29. Zarrinfar H, Kaboli S, Dolatabadi S, *et al*. Rapid detection of Candida species in bronchoalveolar lavage fluid from patients with pulmonary symptoms. Braz J Microbiol 2016; 47: 172-176.
30. Fontana C, Gaziano R, Favaro M, *et al*. (1-3)-beta-D-glucan vs galactomannan antigen in diagnosing invasive fungal infections (IFIs). Open Microbiol J 2012; 6: 70-73.

Experience in Training an Artificial Intelligence Model for Lung Nodule Detection

Chih-Hsiung Chen[1], Kuang-Yu Hsieh[1], Kuo-En Huang[1]

Background: The mainstream approach in artificial intelligence (AI) training using chest X-rays (CXRs) focuses on pneumonia detection. This study adopted a TensorFlow-based model to run on a home computer, utilizing a publicly available dataset designed for pulmonary nodule detection. The objective was to train an AI model to identify pulmonary nodules.

Methods: The dataset from the Japanese Society of Radiological Technology (JSRT) comprises 247 CXRs, including 154 images with nodules and 93 without nodules. For training, the dataset was divided into a training set for training and a test set for model validation. The AI model was adopted from Ethan Chapman's architecture designed for pneumonia detection. Upon achieving successful training, the model's performance was evaluated using the area under the receiver operating characteristic curve (AUROC).

Results: We trained a pulmonary nodule detection model on a home computer. After 1,000 training epochs, the loss converged toward 0.5 without divergence, and the model's accuracy stabilized within the range of 0.9 to 0.95. The model's AUROC achieved a score of 0.77.

Conclusion: The final results revealed moderate performance compared to pneumonia detection reported in previous literature. Our work broadens the scope of AI applications in pneumonia detection and offers valuable experience for AI training in medical imaging. ***(Thorac Med 2026; 41: 23-31)***

Key words: AI training, medical imaging, pneumonia, pulmonary nodule, TensorFlow

Introduction

The introduction of large language models (LLMs) and diffusion models in 2022 marked a remarkable leap forward in Artificial Intelligence (AI). Beyond generative imaging, LLMs such as OpenAI's GPT [1], Google's Gemini [2], and Anthropic's Claude [3] have been rapidly adopted across diverse domains within just 1 to 2 years. While LLMs have demonstrated significant success in medical text and language processing, their progress in medical imaging has been comparatively limited.

The slower advancement in medical imaging AI can be attributed to several factors. First, dataset preparation requires time-consuming annotation and extensive data retrieval and processing. Institutional Review Board (IRB)

[1]Division of Critical Care Medicine, Mennonite Christian Hospital, Hualien, Taiwan.
Address reprint requests to: Dr. Kuo-En Huang, Department of Critical Care Medicine, Mennonite Christian Hospital, Hualien, Taiwan.

approval, which is crucial for safeguarding research participants, is both time-intensive and resource-demanding. Additionally, training AI models for medical imaging requires large datasets, and obtaining sufficient informed consent poses a significant challenge. Even after acquiring these datasets, annotating medical images to create usable training data requires the expertise of skilled physicians with domain-specific knowledge. As a result, much of AI training in medical imaging relies on publicly available datasets. Consequently, introductory research in this field often focuses on pneumonia detection [4-7].

Detection of pulmonary nodules is a critical topic in chest medicine. In this study, we utilized a chest X-ray (CXR) dataset provided by the Japanese Society of Radiological Technology (JSRT), specifically designed for binary classification, to determine the presence or absence of nodules [8]. Using this dataset, we developed a straightforward binary classification model and now would like to share our experience as a foundational reference for future researchers.

Material and Methods

1. Japanese Society of Radiological Technology (JSRT) Dataset

The dataset used in this study was provided by the JSRT [8] and consisted of 247 chest X-rays. This publicly available database includes posteroanterior chest radiographs collected from 13 institutions in Japan and 1 in the United States. Of the 247 images, 154 contain nodules of various sizes, and 93 are labeled as normal, without nodules. As of February 19, 2021, this dataset had been available to researchers worldwide for 24 years and had been cited 326 times in the Web of Science Core Collection, including 191 journal articles, 123 conference proceedings, 15 review papers, and 7 book chapters [9]. The dataset is accessible for downloading from the following 2 websites:

A. The JSRT website

The JSRT dataset is available online at http://db.jsrt.or.jp/eng.php. To download the dataset, users must first register as members. Once registered, access to the dataset is granted via http://db.jsrt.or.jp/eng-04.php, where the dataset is listed in the "Digital Image Database" category in the "Resources" section of the menu. The total storage size for all 247 images is 1.33 gigabytes, with the nodule cases (154 images) occupying 809.94 megabytes and the non-nodule cases (93 images) requiring 487.47 megabytes. The dataset also includes 2 supplementary files, DB_UsersGuide2008.pdf (145 kilobytes) and Clinical_Information.zip (5 kilobytes). The image files were generated using the Konica LD 4500 and LD 5500 Film digitizers. The image parameters are 2048 x 2048 in matrix size, 0.175 millimeters in pixel size, and 4096 (12 bits) in gray levels, with an optical density range from 0.0 to 3.5, and with higher optical density corresponding to higher pixel values, and lower density to lower pixel values.

B. The Kaggle website

Another access point for the JSRT dataset is available on the Kaggle platform at https://www.kaggle.com/datasets/raddar/nodules-in-chest-xrays-jsrt. Kaggle, a widely recognized platform in the AI community, hosts a variety of datasets to promote AI applications, including a mirrored download of the JSRT dataset. One key advantage of the Kaggle version is that the image data is provided in the commonly used '.png' format, converted from the original dataset. This facilitates straightforward access using standard image processing software and seam-

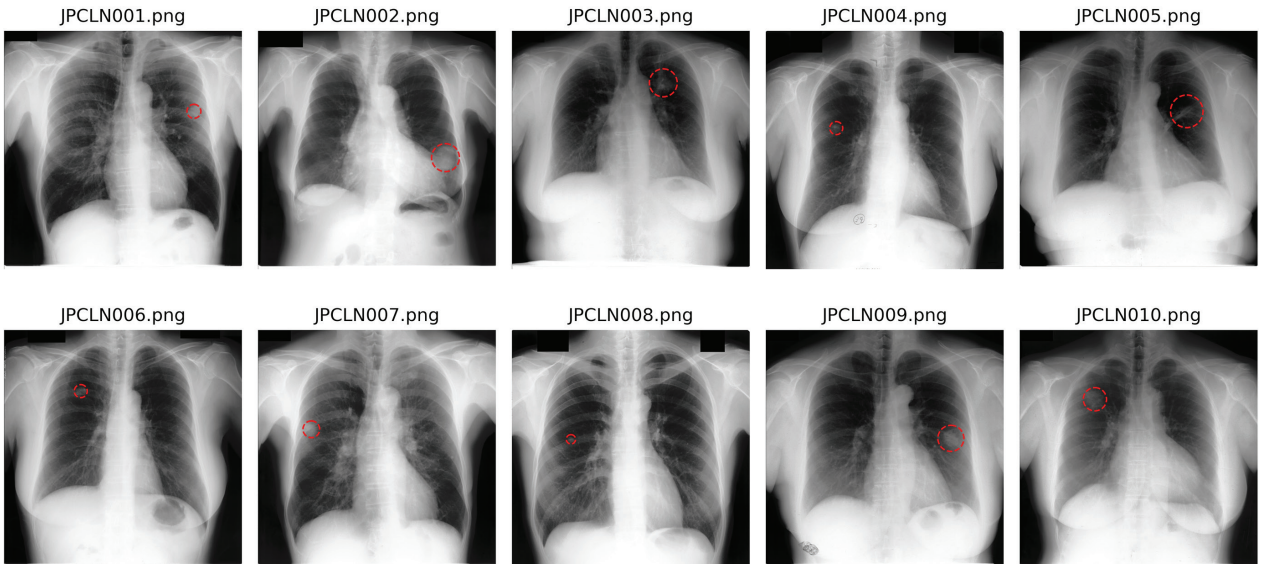

Fig. 1. Illustration of images with nodule lesions.
The files labeled as JPCLN***.IMG represent images containing lung nodules. The associated information for these images includes the filename, degree of subtlety, nodule size in millimeters, patient age and gender, x and y coordinates of the nodule location within the image, malignant or benign classification, anatomic location, and final diagnosis. The figure displays the first 10 images from the dataset, with dashed circles marking the locations of the nodules. Larger lesions are highlighted with larger dashed circles, while smaller lesions are marked with proportionally smaller circles. During the training process, these dashed circles were not included in the images.

less integration with popular Python libraries such as OpenCV and matplotlib, eliminating the need for additional format conversions. Furthermore, the original JSRT metadata files include tab byte characters '\t', which can cause issues during data parsing and often require manual formatting adjustments. Kaggle addresses this limitation by offering a preprocessed metadata file 'jsrt_metadata.csv' for easy reference. For these reasons, this study primarily utilized the Kaggle dataset, leveraging its preformatted '.png' images and clean metadata to streamline the analysis process.

C. JRST meta information

For the lung nodule images (JPCLN***.IMG), clinical data and information are arranged in the order of image filename, degree of subtlety, nodule size in millimeters, age, gender, x and y coordinates of the nodule location in the image, whether malignant or benign in pathology, anatomic location, and final diagnosis. For image files without nodule information (JPCNN***.IMG), clinical data are organized in the following order: image filename, age, gender, and diagnosis, all of which are denoted as non-nodule. See Fig. 1 below.

2. Model Development

Our model builds upon the approach developed by Ethan Chapman in 2021. The original code and detailed explanations are available at https://oak-tree.tech/blog/xray-classification-tensorflow2. In his work, Ethan Chapman created a binary classification model to detect the presence or absence of pneumonia. We adopted his architecture and modified the code to classify the presence of nodules in our study.

A. Dataset sets

The JSRT dataset is divided into a training set and a test set. The training set includes 138

images with nodule lesions and 81 images without nodules, while the test set, used to validate the model's accuracy, consists of 15 images with nodule lesions and 12 images without nodules.

B. Model architecture

This model based on Tensorflow is a convolutional neural network designed for binary classification tasks, starting with an input layer that accepts single-channel grayscale images, with images 150 x 150. It incorporates multiple 2D convolutional layers to process image features, each utilizing a kernel size of (3, 3) and the ReLU activation function. The padding parameter is set to 'same' to ensure that the spatial dimensions of the feature maps remain unchanged. To reduce the size of the feature maps and extract key features, max pooling layers are added after every 2 convolutional layers, using a (2, 2) window and stride. Batch normalization layers are included to stabilize the training process and improve convergence speed.

After feature extraction, the feature maps are flattened and passed through 2 fully connected layers. The first dense layer contains 256 units with ReLU activation, followed by a second dense layer with 128 units and ReLU activation. To reduce the risk of overfitting, a 20% dropout layer is applied after the dense layers. The model concludes with a single-neuron output layer that uses a Sigmoid activation function, mapping the output to the range [0, 1], which is suitable for binary classification. Table 1 below provides the layer's summary.

C. Training

We deployed the model to a desktop computer running the Microsoft Windows 11 platform. The software environment includes Python 3.10 with TensorFlow 2.10.1. The hardware configuration features an RTX 3060 Graphics Processing Unit (GPU) with 6 gigabytes of memory, and the CUDA version is 11.8.r11.8.

The model uses the RMSprop optimizer, which adjusts the learning rate dynamically for each parameter, making it well-suited for handling non-stationary objectives. Binary_crossentropy loss is used, which is appropriate for binary classification tasks where the output is in the range [0, 1]. The model tracks accuracy as a performance metric during training, which evaluates the percentage of correctly classified samples.

The model is trained using datagen.flow(), which generates augmented data batches on-the-fly from the training dataset (X_train and y_train). This helps improve model generalization by creating variations of the input data. Training is conducted in size-32 mini batches to efficiently process data and update model parameters. Data is shuffled at each epoch to ensure the model doesn't learn patterns based on the order of the data. The training process runs for 1000 epochs, meaning the model iterates over the entire training dataset 1000 times. The loss and accuracy during training were stored for statistics each epoch, which can be used for visualization or further analysis.

3. Validation and Evaluation

After training the model, we used the test dataset, which was denoted as the X_test and y_test, to validate the model's performance. Upon completing the validation, we evaluated the model using the Area Under the Receiver Operating Characteristic Curve (AUROC). The AUROC measures the model's ability to distinguish between classes across different thresholds. A higher AUROC value indicates better discrimination capability, with a value of 1.0 representing perfect classification and 0.5 indicating no

Table 1. Summary of Layers in the Model.

Model: "sequential"		
Layer (type)	Output Shape	Param #
Conv2D	(None, 150, 150, 64)	640
Conv2D	(None, 150, 150, 64)	36928
MaxPooling2D	(None, 75, 75, 64)	0
BatchNormalization	(None, 75, 75, 64)	256
Conv2D	(None, 75, 75, 128)	73856
MaxPooling2D	(None, 37, 37, 128)	0
BatchNormalization	(None, 37, 37, 128)	512
Conv2D	(None, 37, 37, 256)	295168
MaxPooling2D	(None, 18, 18, 256)	0
BatchNormalization	(None, 18, 18, 256)	1024
Conv2D	(None, 18, 18, 256)	590080
MaxPooling2D	(None, 9, 9, 256)	0
BatchNormalization	(None, 9, 9, 256)	1024
Conv2D	(None, 9, 9, 512)	1180160
MaxPooling2D	(None, 4, 4, 512)	0
Flatten	(None, 8192)	0
Dense	(None, 256)	2097408
Flatten	(None, 256)	0
Dense	(None, 128)	32896
Dropout	(None, 128)	0
Dense	(None, 1)	129
Total params: 4,310,081		
Trainable params: 4,308,673		
Non-trainable params: 1,408		

The model consists of 3 main components. The first part processes input images through 2 Conv2D layers, followed by 4 consecutive ensemble blocks. Each ensemble block includes MaxPooling2D, BatchNormalization, and Conv2D layers, progressively reducing the spatial dimensions to one-fourth of their original size while doubling the number of channels. Then, the initial 150x150 grayscale input is transformed into a 4x4 representation with 512 channels. The output of the second part is flattened and fed into fully connected layers. Finally, a Dense layer maps the output to the range [0, 1], providing probability values

better than random guessing. This metric is particularly useful for assessing imbalanced datasets, as it provides an aggregated measure of performance across all classification thresholds.

Results

After training the model for 1000 epochs, it was evident that as the number of epochs increased, the loss values gradually decreased, as shown in Figure 1. Apart from the relatively high loss values observed at the beginning of training, the overall trend showed a continuous reduction in loss, indicating the model's improvement during training. Meanwhile, the accuracy progressively improved and eventually plateaued, reaching a stable value over time, as illustrated in Fig. 2. This indicates that the model effectively learned from the training data and achieved a point of convergence where further training resulted in minimal performance gains. The overall accuracy stabilized between

approximately 1.0 and 0.9. The consistent reduction in loss and the stabilization of accuracy demonstrated the effectiveness of the training process.

Immediately after training, we validated the model using the test dataset. The images from the test dataset were input into the model for predictions, and the predicted values were compared with the true labels to generate an AUROC. Following these steps, the final AUROC obtained was 0.77. We set the threshold to 0.5, and the calculated F1-score to be 0.6923.

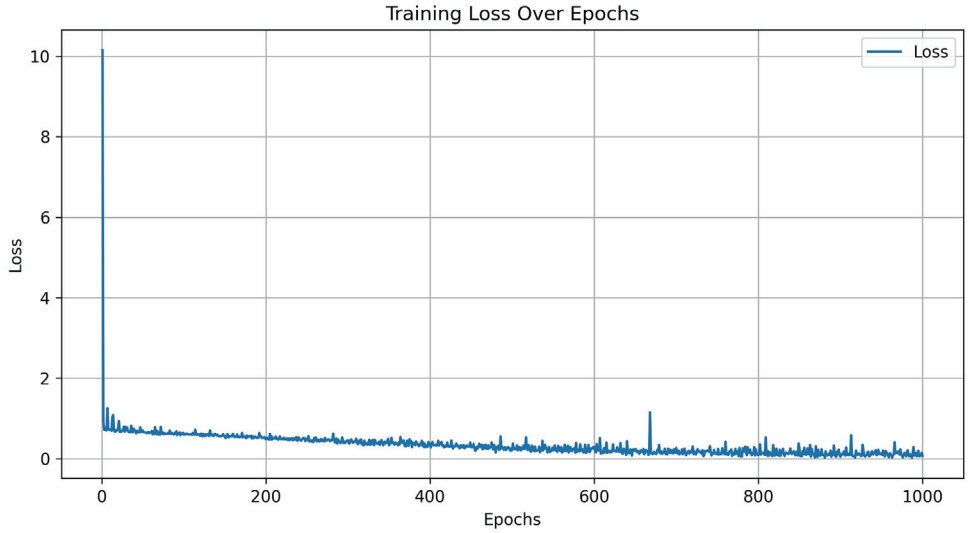

Fig. 2. Training loss over epochs.
In this figure, it can be observed that, aside from the initially high loss, the loss gradually decreased during the later stages of training. Only a few spikes occurred, but these did not affect the overall loss trend. At around 600 epochs, the loss converged to below 0.5.

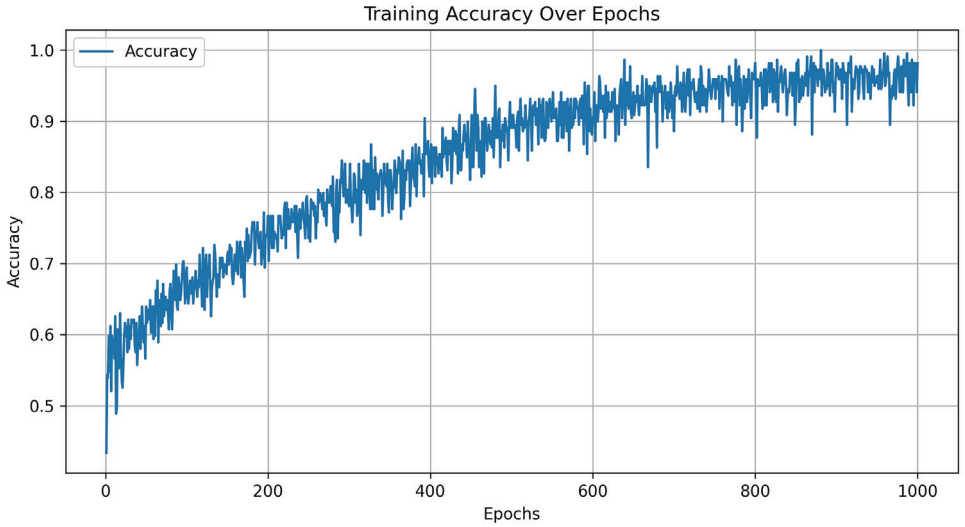

Fig. 3. Training accuracy over epochs.
This is the accuracy graph after 1000 epochs of training. As shown in the figure, accuracy starts climbing from 0.5 and stabilizes between 1.0 and 0.9 at around the 600th epoch, without any further significant increase. The lack of further improvement may indicate that the model has not yet shown signs of overfitting, suggesting that it is generalizing well to the training data.

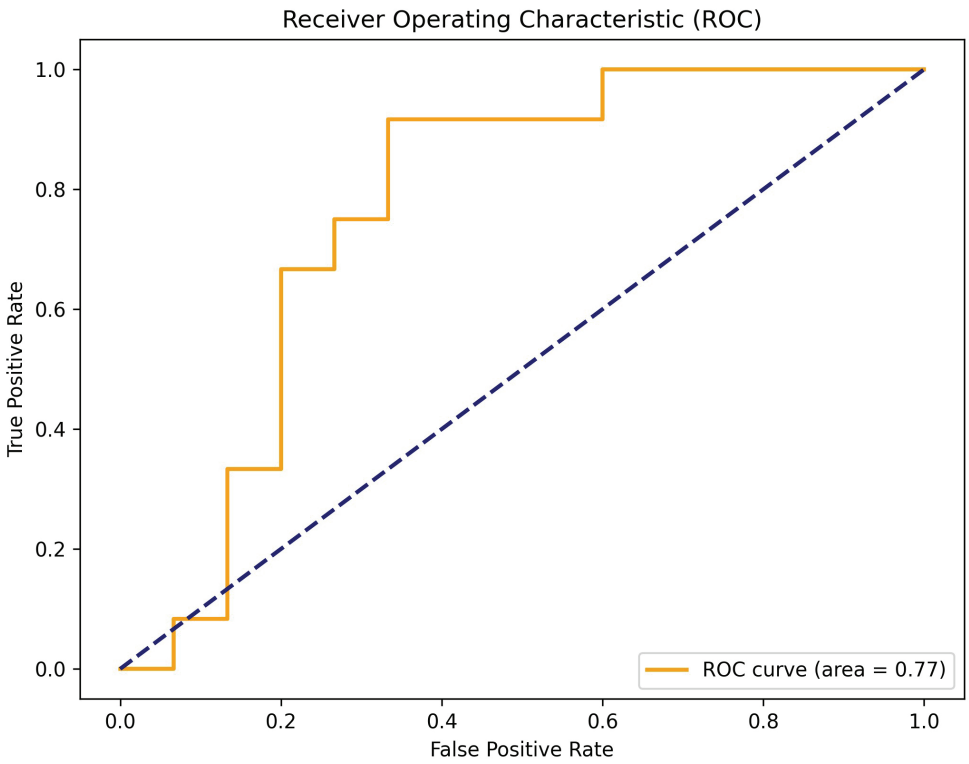

Fig. 4. The area under the receiver operating characteristic curve.
The jagged appearance of the curve is related to the number of cases in the test dataset. Increasing the number of cases in the test dataset could result in a smoother curve. The AUROC was 0.77.

Discussion

Entering the field of AI use for medical applications comes with notable challenges. Beyond the difficulty of obtaining suitable datasets for training, another major hurdle lies in the complexity of AI programming, which is not as straightforward as traditional programming. Additionally, AI training often requires substantial computational power [10]. These challenges may deter medical professionals who are eager to learn AI. Based on our research experience, we hypothesize that migrating AI training to personal computers can not only increase willingness to learn but also allow users to modify models according to their ideas, enabling validation of model accuracy at any time.

The 2 most often used frameworks for AI development are TensorFlow and PyTorch. TensorFlow was developed by Google AI Group [11], while PyTorch is a product of Meta (formerly Facebook AI Group) [12]. Of these 2, TensorFlow is considered to have a lower barrier to entry. Although most mainstream LLMs are built on the PyTorch framework, the majority of medical image AI training relies on TensorFlow. In this study, we adopted TensorFlow as the primary framework, modifying an existing pneumonia diagnosis model to detect nodules using a different dataset. The modified code was suc-

cessfully implemented on a personal computer.

There is limited research on entry-level or demonstration programs for chest X-ray medical imaging, and most focus on pneumonia diagnosis. This may be due to the availability of publicly accessible datasets, which are predominantly centered around pneumonia detection. For instance, the model architecture modified in this study, known as the Ethan Chapman model, was developed based on the pneumonia dataset provided by Kermany DS, *et al.* [13]. They collected and labeled 5,232 chest X-ray images from children, including 3,883 images depicting pneumonia (2,538 bacterial and 1,345 viral) and 1,349 normal images, from a total of 5,856 patients, to train their AI system. The model was subsequently tested with 234 normal images and 390 pneumonia images (242 bacterial and 148 viral) from 624 patients. The AUROC for pneumonia detection achieved an impressive 96.8% [14].

This AUROC value is higher than the 77% achieved in our nodule lesion detection task. We believe this discrepancy is primarily due to the larger affected areas in pneumonia cases. Despite downscaling the original images to 299×299 with 3 channels, the model could still detect pneumonia effectively. Furthermore, the number of cases in Kermany's dataset far exceeds that of the JSRT dataset used in our study. The smaller dataset size is likely another contributing factor to the lower AUROC in our nodule lesion detection.

Unlike previous studies that relied solely on accuracy to evaluate training outcomes, we introduced AUROC to assess our model. AUROC is a crucial metric for evaluating the performance of binary classification models, especially in scenarios requiring a balance between sensitivity and specificity, such as medical diagnoses and disease detection. AUROC measures a model's ability to correctly classify positive and negative cases across different thresholds. Its value ranges from 0 to 1, where values closer to 1 indicate better performance. An AUROC of approximately 0.5 suggests a performance equivalent to random guessing, while an AUROC > 0.7 indicates reasonable discriminatory power, and an AUROC = 1.0 represents a perfect classification model. Our model demonstrates a certain level of recognition capability, highlighting its potential for binary classification in medical applications.

Limitations

The JSRT nodule dataset categorizes nodules into 5 levels of difficulty based on diagnostic complexity, with level 1 being the most challenging and level 5 the easiest. When identifying lung nodules, factors such as the location of the nodule and its size significantly influence interpretation. In this study, the JSRT images provided were 2048 x 2048 grayscale. To make the training process compatible with desktop computers and general-purpose GPUs, we downscaled the image size to 150 x 150 grayscale. For smaller lesions, this reduction in resolution could lead to certain nodules, already small, becoming even smaller and indistinguishable from background noise, making them harder to detect.

The current training approach involves feeding the entire CXR image into the model. Previous studies have suggested that for smaller lesions, cropping specific regions of interest may enhance detection accuracy [15], and this could be a direction for future research. Lastly, due to the lack of additional datasets for external validation, the applicability of the results

from the test dataset used in this study to other types of datasets remains uncertain. This represents a limitation of our research.

Conclusions

After analyzing the JSRT nodule dataset, we successfully applied it to train a neural network model for pulmonary nodule detection. This study modified an AI model originally designed for pneumonia detection and adapted it for pulmonary nodule detection. For beginners in neural network learning, this work provides an additional example of lesion detection beyond pneumonia. While the final training results were somewhat modest, we believe that increasing the number of cases in the dataset could further enhance the model's detection capabilities.

References

1. Radford A, Narasimhan K, Salimans T, *et al*. Improving language understanding by generative pre-training. OpenAI preprint 2018; https://cdn.openai.com/research-covers/language-unsupervised/language_understanding_paper.pdf
2. Chowdhery A, Narang S, Devlinet J, *et al*. PaLM: scaling language modeling with pathways. arXiv 2022; 10.48550/arXiv.2204.02311
3. Bai Y, Kadavath S, Kundu S, *et al*. Constitutional AI: harmlessness from AI feedback. arXiv 2022; 10.48550/arXiv.2212.08073
4. Rajpurkar P, Irvin JA, Ball RL, *et al*. Deep learning for chest radiograph diagnosis: a retrospective comparison of the CheXNeXt algorithm to practicing radiologists. PLoS Med 2018; 15:e1002686.
5. Bhandari M, Shahi TB, Siku B, *et al*. Explanatory classification of CXR images into COVID-19, pneumonia and tuberculosis using deep learning and XAI. Comput Biol Med 2022; 150: 106156.
6. Santosh KC, Allu S, Rajaraman S, *et al*. Advances in deep learning for tuberculosis screening using chest X-rays: the last 5 years review. J Med Syst 2022; 15: 46: 82.
7. Subramanian N, Elharrouss O, Al-Maadeed S, *et al*. A review of deep learning-based detection methods for COVID-19. Comput Biol Med 2022; 143: 105233.
8. Shiraishi J, Katsuragawa S, Ikezoe J, *et al*. Development of a digital image database for chest radiographs with and without a lung nodule: receiver operating characteristic analysis of radiologists' detection of pulmonary nodules. AJR Am J Roentgenol 2000; 174(1): 71-4.
9. JSRT database introduction at Japanese Society of Radiological Technology website: http://db.jsrt.or.jp/eng.php.
10. Sastry G, Heim L, Belfield H, *et al*. Computing power and the governance of artificial intelligence. arXiv 2024; 10.48550/arXiv.2402.08797
11. Abadi M, Barham P, Chen J, *et al*. TensorFlow: a system for large-scale machine learning. arXiv 2016; 10.48550/arXiv.1605.08695
12. Paszke A, Gross S, Massa F, *et al*. PyTorch: an imperative style, high-performance deep learning library. arXiv 2019; 10.48550/arXiv.1912.01703
13. Kermany D, Zhang K, Goldbaum M. Labeled optical coherence tomography (OCT) and chest X-ray images for classification. Mendeley Data 2018; 10.17632/rscbjbr9sj.2
14. Kermany DS, Goldbaum M, Cai W, *et al*. Identifying medical diagnoses and treatable diseases by image-based deep learning. Cell 2018; 172(5): 1122-1131.
15. Chen CH, Hsu SH, Hsieh KY. *et al*. The two-stage detection-after-segmentation model improves the accuracy of identifying subdiaphragmatic lesions. Sci Rep 2024; 14: 25414.

Endobronchial Ultrasound-Guided Cryobiopsy in the Diagnosis of Primary Pulmonary Lymphoma: Case Report of a Novel Application

Yu-Hua Su[1], Chia-Hung Chen[1,2], Yu-Chang Fu[1], Chih-Yen Tu[1,2]

Primary pulmonary lymphomas (PPLs) are rare lung malignancies, and their diagnosis requires large amounts of tissue via open lung biopsy. A prompt diagnosis is vital, as PPLs are highly responsive to chemotherapy, and complete remission is possible. Cryobiopsy with endobronchial ultrasound guidance (EBUS-cryobiopsy) can provide significantly larger amounts of tissues than standard percutaneous CT-guided and traditional transbronchial forceps biopsies. Herein, we report a 66-year-old female who presented with an asymptomatic and incidental mass-like lesion in the right lower lung. Tissues from CT-guided needle and EBUS-guided traditional forceps biopsies failed to yield a specific diagnosis, whereas those from EBUS-guided cryobiopsy confirmed the diagnosis of PPL. This case indicates that cryobiopsy can be used to diagnose PPLs, especially when large amounts of tissue are required, and that it may be an alternative to open lung biopsy in certain cases. ***(Thorac Med 2026; 41: 32-38)***

Key words: Cryobiopsy, forceps biopsy, primary pulmonary lymphoma

Introduction

Lymphomas can involve the lungs through hematogenous dissemination, contiguous spread through mediastinal structures, or primary pulmonary involvement [1-2, 17]. Primary pulmonary lymphomas (PPLs) are exceedingly rare entities (0.5-1% of all primary pulmonary malignancies) and can be defined as malignant monoclonal lymphoid proliferations localized to the lungs, in the absence of any extra-thoracic involvement detected within 3 months following the intial diagnosis [1-2, 17]. The symptoms and radiographic findings of PPLs are nonspecific and may initially be misdiagnosed as other pulmonary diseases, such as pneumonia, tuberculosis, or lung cancer [14].

Tissue sample size is crucial for establishing the diagnosis of pulmonary lesions that diffusely involve the lung parenchyma or interstitium [3]. Among these diseases, lymphoma has a complex histopathologic background, and

[1]Division of Pulmonary and Critical Care Medicine, Department of Internal Medicine, China Medical University Hospital, [2]School of Medicine, China Medical University.
Address reprint requests to: Dr. Chia-Hung Chen, Department of Internal Medicine, China Medical University Hospital, No. 2, Yude Road, Taichung, Taiwan.

the limited tissue obtained from biopsy may hinder advanced investigations—such as immunohistochemistry and molecular analyses—that are essential for establishing a definitive diagnosis and accurately identifying the disease classification and subtype [15]. Traditionally, open lung biopsy has been the standard method for diagnosing PPLs [4, 16]. However, with the development of high-resolution computed tomography (CT) enhancing clinico-pathological correlation, along with the introduction of molecular diagnostic tools, less invasive techniques such as bronchoscopic transbronchial biopsy, bronchoalveolar lavage, and fine-needle aspiration have become more commonly used. Despite their utility, these methods frequently fail to provide sufficient tissue for a definitive diagnosis of PPLs [16].

Cryobiopsy has been shown to significantly increase the diagnostic yield, compared with conventional forceps biopsy, by obtaining larger tissue specimens [6, 16], although it has been associated with higher rates of bleeding and pneumothorax in some series [7]. We report the case of a 66-year-old woman with PPL without pulmonary symptoms who underwent CT-guided biopsy and endobronchial ultrasound (EBUS)-guided forceps biopsy which only yielded inconclusive diagnoses. Finally, EBUS-guided cryobiopsy revealed pathological findings suggesting diffuse large B-cell lymphoma.

Case Presentation

A 66-year-old female nonsmoker presented with acute onset of right upper quadrant abdominal pain for 1 week. She also complained of nausea and anorexia, but fever, cough and dyspnea were not noted. On presentation, she was ambulatory and not in any distress. Auscultation revealed clear breathing sounds. The abdomen was tender to palpation on the right upper quadrant. Abdominal ultrasound showed a mildly dilated common bile duct with gallstones, and chest X-ray showed an ill-defined opacity in the right lower lung (RLL) region (Fig. 1). An abdominal CT scan revealed cholecystitis and an RLL tumor. She immediately underwent percutaneous gallbladder drainage for cholecystitis. We arranged a CT-guided biopsy of the RLL tumor, but the final histopathologic report was chronic inflammation without malignancy. Due to lack of a definite diagnosis of the CT-guided biopsy specimen, she received a radial probe EBUS-guided biopsy for the RLL tumor, which showed a lesion enclosing the radial EBUS probe (Fig. 2). However, the final histopathologic diagnosis was still chronic inflammation, with no malignancy. Bacterial culture, fungal culture and acid-fast staining of the bronchoalveolar lavage specimen also yielded negative results.

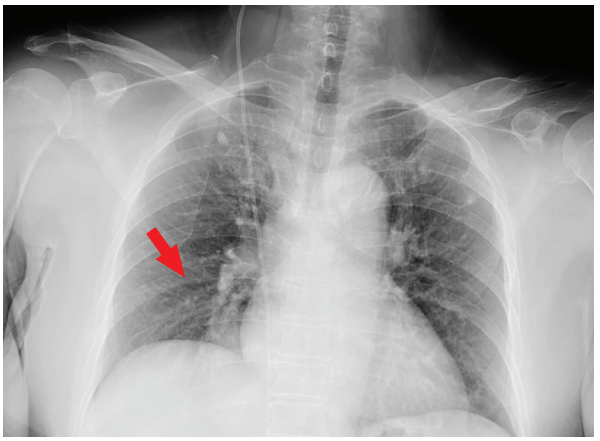

Fig. 1. Initial chest X-ray after the patient presented with abdominal pain, showing only minimal hazy opacity in the right lower lung region.

The patient's presentation with the CT images and histopathologic findings suggested possible organizing pneumonia. Oral clarithromycin was administrated for 8 weeks as an im-

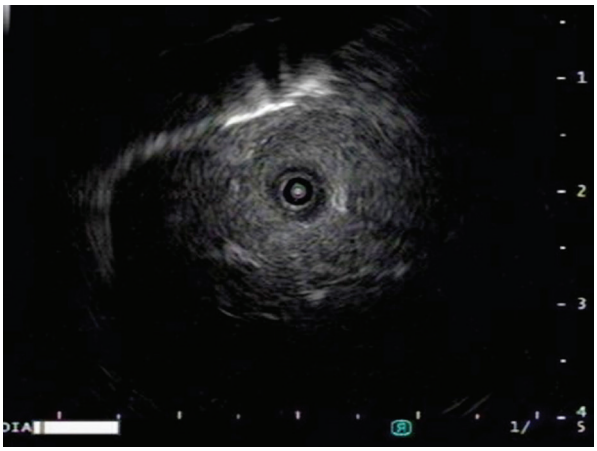

Fig. 2. Patient's initial EBUS image demonstrating a type III (heterogeneous) "within" lesion, indicative of a high likelihood of malignancy.

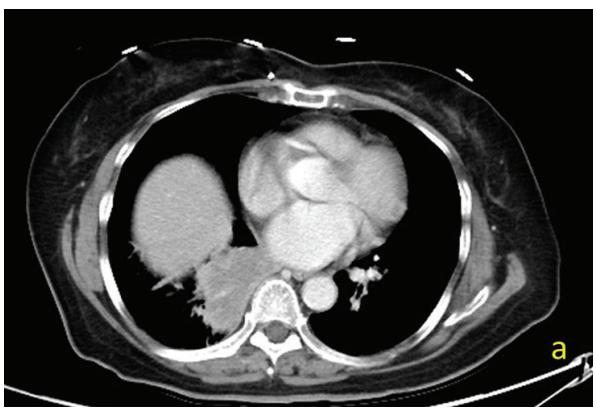

Fig. 3a. Initial abdominal CT scan with portions of the lower lungs visible.

Fig. 3b. Follow-up chest CT scan performed after empiric treatment with clarithromycin. The medial portion of the lesion has resolved and the lateral portion has markedly progressed, despite treatment.

munomodulatory agent. A follow-up CT was performed 3 months after the initial CT scan and after the empiric clarithromycin treatment. The findings of the new CT scan showed resolution of the infiltrations on the medial side but progression of the lesion in the lateral segment of the lower lobe (Fig. 3). Malignancy was highly suspected due to the minimal response to empiric treatment. A surgical lung biopsy was suggested, but she refused, so a repeat radial probe EBUS-guided cryobiopsy was considered.

The repeat EBUS-guided forceps biopsy and cryobiopsy were performed 3 months after the initial presentation. The conventional forceps biopsy samples measured 0.2x0.1x0.1 cm, and histopathology showed acute and chronic inflammation of the RLL with mixed neutrophils, lymphocytes and foamy histiocytic aggregation. No malignancy was seen in the forceps biopsy samples.

The cryobiopsy samples measured 0.4x0.3x0.3 cm (Fig. 4), and the final histopathology revealed heavy lung infiltration with medium-sized atypical lymphoid cells with angulated nuclei and focal necrosis. Immunohistochemistry was positive for CD10, CD20, bcl-6 and MUM-1 (focal), and negative for CD3, CD56, cyclin D1 and EBER-ISH. A diagnosis of malignant lymphoma, favoring germinal center-type diffuse large B-cell lymphoma, was established.

Despite the apparent delay in the final diagnosis, PPL was confirmed through the use of EBUS-guided cryobiopsy. No procedure-related complications, including bleeding, pneumothorax, or hypoxia, were observed. Positron-emission tomography confirmed that the lesion was confined to the lung, with no nodal or distant metastases (Fig. 5).

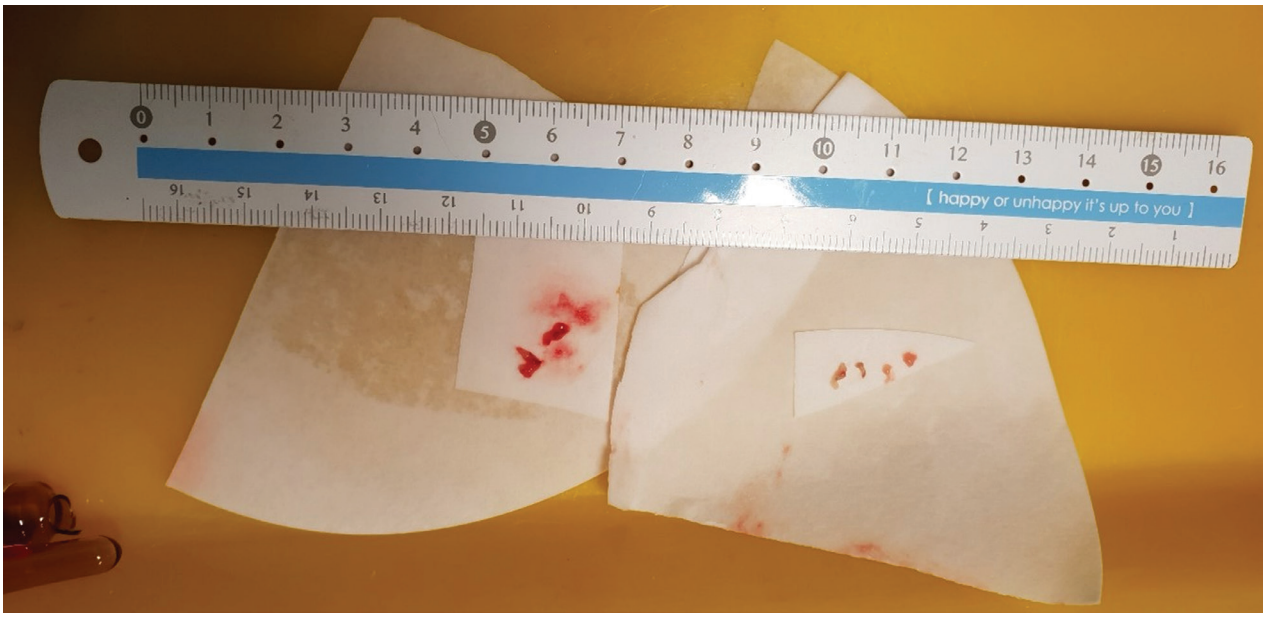

Fig. 4. The cryobiopsy specimens were significantly larger (left side) than the conventional forceps biopsy specimens (right side).

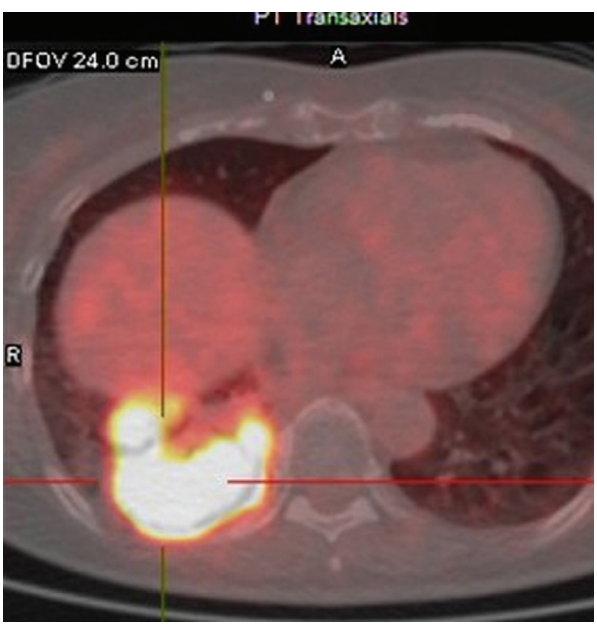

Fig. 5. PET image confirms a PET-avid malignancy confined to the right lower lobe with no nodal and distant spread.

Discussion

PPLs pose a diagnostic challenge due to their atypical presentation and the absence of specific clinical and radiographic findings. Further diagnostic approaches, such as biopsy, should be initiated when imaging findings are inconsistent with the clinical symptoms or when there is a lack of response to the initial treatment based on the presumed diagnosis [14]. As in our case, the patient was initially misdiagnosed with organizing pneumonia. However, follow-up imaging after macrolide treatment revealed lesion progression, raising strong suspicion of an alternative diagnosis and required further tissue biopsy.

The main challenge of our case was to obtain an adequate and sufficient tissue specimen to diagnose the radiographic abnormality. With no clues of underlying lymphoma, the most prudent approach initially was the least invasive procedure, however these procedures (CT-

guided needle biopsy, and EBUS conventional forceps biopsy) failed to reveal the proper histologic diagnosis. When the initial medical treatment failed, we suggested surgical biopsy. As the patient declined the surgery, we subsequently proposed radial probe EBUS-guided cryobiopsy, considering that cryoprobe use involves self-payment.

Surgical lung biopsy remains the gold standard to diagnose lung lesions that require large amounts of tissue. It has the advantage of direct visualization and palpation of the lesion, and sampling of the distal lung parenchyma. However, surgical lung biopsy carries higher risks of morbidity and mortality, incurs greater costs, and often results in a longer hospital stay. Furthermore, the likelihood of procedure-related complications, such as pneumothorax and bleeding, is increased [18-19]. In addition, in patients with multiple comorbidities or compromised clinical status, surgery may not be well tolerated [16].

Bronchoscopy with cryobiopsy has been shown to be able to obtain significantly larger amounts of tissue, compared to conventional forceps biopsy, to diagnose focal lung lesions [8], malignancy, and diffuse parenchymal and interstitial abnormalities [9], and for sampling pleural lesions in medical pleuroscopy [10]. Obtaining greater amounts of tissue is beneficial for establishing a definitive diagnosis, as it allows for additional immunohistochemical and molecular analyses. Moreover, in cases of epithelial cancers (particularly adenocarcinoma), retrieving greater tissue samples is recommended, since Next Generation Sequencing (NGS) has become a standard part of the diagnostic process [15]. Transbronchial lung cryobiopsy can be considered a valid alternative to surgical lung biopsy, offering an adequate diagnostic yield with a lower complication rate [16]. Bronchoscopy with cryobiopsy is more suitable for some vulnerable patients and may provide cost savings for our healthcare system [20].

Controversy exists over whether cryobiopsy is non-inferior to surgical lung biopsy in terms of yield for interstitial and diffuse parenchymal lung diseases [11-12]. No controlled studies have examined the utility of EBUS cryobiopsy in the diagnosis of pulmonary malignancies that require a large amount of tissue. Our case successfully illustrated the utility of an EBUS cryobiopsy compared to other methods of biopsy in the diagnosis of a rare pulmonary malignancy. In specific clinical scenarios, such as suspected lymphoma or when a large amount of tissue is required for further examinations like NGS, cryobiopsy may be considered as an initial diagnostic approach due to its relatively less invasive nature, provided that the patient does not have contraindications such as hemodynamic instability, pulmonary hypertension, uncorrected bleeding tendency, severe hypoxemia, pregnancy, or diffuse lung disease with extensive cysts or bullae [21]. Open lung biopsy can serve as a salvage option in cases where cryobiopsy fails or as an alternative for economically disadvantaged patients in Taiwan.

The timely diagnosis of pulmonary malignancy is of paramount importance since early-stage malignancies are potentially curable. PPLs are especially responsive to current chemotherapy and immunotherapy regimens with monoclonal antibodies, and the prognosis with treatment is excellent in early stages [1, 8]. Despite the delay in obtaining tissue for the diagnosis in our case, the patient's lymphoma remained confined to the lungs. This case highlights that a rapid and accurate diagnosis is essential for a potentially curable pulmonary

malignancy. There is a wide gap in our medical knowledge regarding which patient groups should be offered cryobiopsy as a first-line diagnostic tool to increase yield, and our report may provide an insight into this question.

Conclusions and Recommendations

Lung cryobiopsy shows potential as a new tool in the diagnosis of various rare lung tumors and other lung pathologies that require large tissue samples for an accurate diagnosis. Our case highlights the advantages of EBUS-cryobiopsy over other forms of lung biopsy. This report may shed light on and prompt future research into which specific groups of patients may warrant cryobiopsy as the diagnostic tool of choice to maximize yield, minimize complications, and optimize cost-effectiveness.

References

1. Cadranel J, Wislez M, Antoine M. Primary pulmonary lymphoma. Eur Respir J 2002; 20(3): 750-62.
2. Shen MF, Ju TR, Lee CC, *et al*. Novel application of cryobiopsy in the diagnosis of pulmonary alveolar proteinosis. Respirol Case Rep 2018 Jun; 6(6): e00336.
3. Lentz R, Argento C, Colby T, *et al*. Transbronchial cryobiopsy for diffuse parenchymal lung disease: a state-of-the-art review of procedural techniques, current evidence, and future challenges. J Thorac Dis 2017 Jul; 9(7): 2186-203.
4. Clagettot AT, Allen TH, Payne WS, *et al*. The surgical treatment of pulmonary neoplasms: a 10-year experience. J Thorac Cardiovasc Surg 1964; 48: 391-400.
5. Kido T, Yatera K, Noguchi S, *et al*. Detection of MALT1 gene rearrangements in BAL fluid cells for the diagnosis of pulmonary mucosa-associated lymphoid tissue lymphoma. Chest 2012; 141(1): 176-82.
6. Yap E, Low I. Bronchoscopic transbronchial cryobiopsy diagnosis of recurrent diffuse large B-cell lymphoma in the lung: a promising new tool? J Bronchol Interv Pulmonol 2017 Apr; 24(2): e22-3.
7. Sethi J, Ali MS, Mohananey D, *et al*. Are transbronchial cryobiopsies ready for prime time?: a systematic review and meta-analysis. J Bronchol Interv Pulmonol 2019 Jan; 26(1): 22-32.
8. Borie R, Wislez M, Thabut G, *et al*. Clinical characteristics and prognostic factors of pulmonary MALT lymphoma. Eur Respir J 2009; 34(6): 1408-16.
9. Babiak A, Hetzel J, Krishna G, *et al*. Transbronchial cryobiopsy: a new tool for lung biopsies. Respiration 2009; 78(2): 203-8.
10. Chen C, Cheng W, Wu B, *et al*. Feasibility and safety of pleuroscopic cryobiopsy of the pleura: a prospective study. Can Respir J 2018 Jan; 6746470.
11. Hagmeyer L, Richter K, Treml M, *et al*. Diagnostic value of transbronchial cryobiopsy compared to surgical lung biopsy. Eur Respir J 2015 (Poster Presentation).
12. Steele M, Benzaquen S, Myers J, *et al*. Cohort comparison between transbronchial cryobiopsy and surgical lung biopsy (SLB) in patients undergoing a workup for interstitial lung disease (ILD) from a multicenter, prospective trial. Am Thorac Soc 2017 (Poster Presentation).
13. Dhooria S, Sehgal I, Aggarwal A, *et al*. Diagnostic yield and safety of cryoprobe transbronchial lung biopsy in diffuse parenchymal lung diseases: systematic review and meta-analysis. Respir Care 2016; 61(5): 700-12.
14. Yao D, Zhang L, Wu PL, *et al*. Clinical and misdiagnosed analysis of primary pulmonary lymphoma: a retrospective study. BMC Cancer 2018; 18: 281.
15. Poletti V, Petrarulo S, Piciucchi S, *et al*. EBUS-guided cryobiopsy in the diagnosis of thoracic disorders. Pulmonology 2024; 30(5): 459-465.
16. Bianchi R, Dubini A, Asioli S, *et al*. Transbronchial cryobiopsy: an effective tool in the diagnosis of lymphoproliferative disorders of the lung. ERJ Open Res 2020; 6(3): 00260-2019.
17. Gozzi L, Cozzi D, Cavigli E, *et al*. Primary lymphoproliferative lung diseases: imaging and multidisciplinary approach. Diagnostics 2023; 13(7): 1360.
18. Shafin Babu PS Sr, Marwah V, Katoch C, *et al*. Diagnostic yield and safety of bronchoscopic lung cryobiopsy in evaluation of lung mass. Cureus 2021; 13(11): e19940.

19. Ravaglia C, Bonifazi M, Wells AU, *et al*. Safety and diagnostic yield of transbronchial lung cryobiopsy in diffuse parenchymal lung diseases: a comparative study versus video-assisted thoracoscopic lung biopsy and a systematic review of the literature. Respiration 2016; 91(3): 215-27.
20. Sharp C, McCabe M, Adamali H, *et al*. Use of transbronchial cryobiopsy in the diagnosis of interstitial lung disease-a systematic review and cost analysis. QJM 2017; 110(4): 207-214.
21. Dhooria S, Agarwal R, Sehgal IS, *et al*. Bronchoscopic lung cryobiopsy: an Indian association for bronchology position statement. Lung India 2019; 36(1): 48-59.

Successful Conservative Management of Tracheal Granulation Tissue Following Tracheostomy: A Case Report

Chun-Chia Chen[1,2], Wen-Kuang Yu[1,2,3]

We reported the case of an 18-year-old female with respiratory failure secondary to a cerebellar hemorrhage who developed circumferential granulation tissue in the middle third of the trachea following tracheostomy. This granulation tissue partially obstructed the airway, particularly during expiration, leading to intermittent acute CO_2 retention that mimicked asthma exacerbations. Conservative management using an extended-length tracheostomy tube was able to effectively bypass the obstruction, and the patient's acute hypercapnia resolved. Gradual resolution of the granulation tissue was confirmed bronchoscopically, without the need for ablative therapies. This case highlights potential tracheostomy complications and underscores the importance of early recognition and non-invasive management to prevent further airway compromise. We included the bronchoscopic findings and clinical course to raise awareness of tracheostomy-related airway complications and support conservative approaches in selected patients. ***(Thorac Med 2026; 41: 39-43)***

Key words: Tracheostomy; tracheal granulation; post-tracheostomy complication

Introduction

Tracheal granulation is a common complication in tracheostomized patients and poses a significant challenge during the weaning process from mechanical ventilation (MV) [1]. This granulation tissue, often resulting from chronic irritation or inflammation at the tracheostomy site, can lead to varying degrees of airway obstruction, further complicating respiratory management. The presence of granulation tissue not only increases airway resistance but also elevates the risk of airway stenosis, prolonging dependence on MV [1-2].

Such complications necessitate interventions, including bronchoscopic evaluations, to assess and restore airway patency. In some cases, advanced therapeutic approaches like ar-

[1]Department of Chest Medicine, Taipei Veterans General Hospital, Taipei, Taiwan. [2]School of Medicine, College of Medicine, National Yang Ming Chiao Tung University, Taipei, Taiwan. [3]Institute of Emergency and Critical Care Medicine, College of Medicine, National Yang Ming Chiao Tung University, Taipei, Taiwan.
Address reprint requests to: Dr. Wen-Kuang Yu, Department of Chest Medicine, Taipei Veterans General Hospital, 201, Section 2, Shih-Pai Road, Taipei, 112, Taiwan.

gon plasma coagulation (APC) or laser therapy are employed to manage granulation tissue effectively and facilitate weaning [3-4]. However, despite these interventions, patients with severe granulation tissue may experience recurrent airflow limitation and bronchospasm, further delaying their ability to achieve spontaneous breathing.

We report the case of a young adult patient with tracheal granulation, which was further complicated by severe wheezing, bronchospasm, and difficulty in weaning from MV. To manage these challenges, we employed an elongation tracheostomy tube along with prolonged ventilatory support and critically supportive care. Frequent bronchoscopy exams allowed us to closely monitor and address airway conditions, resulting in the remarkable resolution of granulation tissue without the need for invasive interventions such as laser therapy or cryotherapy to achieve significant clinical improvement, even in a complex scenario.

Case Presentation

An 18-year-old female with no prior medical history presented with sudden headache, vomiting, and cardiac arrest on November 11, 2023. She underwent 30 minutes of cardiopulmonary resuscitation before return of spontaneous circulation was achieved. Brain computed tomography revealed a large intraventricular hemorrhage (IVH) in the fourth ventricle with obstructive hydrocephalus, necessitating urgent bilateral external ventricular drain placement. Cerebral angiography ruled out vascular malformations, and follow-up magnetic resonance imaging confirmed IVH, subarachnoid hemorrhage, subdural hematoma, and hydrocephalus. Due to persistent ventilator dependence, a tracheostomy was performed on November 28, 2023. Despite transfer for respiratory rehabilitation, weaning attempts failed, and she was referred to our hospital for further management.

On admission, she was conscious and hemodynamically stable. Under physical rehabilitation, her physical examination was unremarkable aside from neurological deficits. She exhibited no significant respiratory distress, and her ventilator settings were gradually adjusted to facilitate weaning. Despite prolonged ventilator dependence, she tolerated rehabilitation sessions well, without desaturation, ventilator asynchrony, or reduction in tidal volume, and no new episodes of bronchospasm were noted, showing some improvement in her general condition.

On June 12, 2024, she developed severe wheezing and bronchospasm, leading to acute desaturation. Bronchoscopy on June 28 revealed circumferential granulation tissue in the mid-trachea, causing luminal narrowing at the tracheostomy opening (Fig. 1). Conservative management with an elongated tracheostomy tube (Bivona® Tracheostomy Tube and Accessories, Smiths Medical, Minneapolis, MN, USA) was preferred over laser or cryotherapy. Despite persistent respiratory difficulties, gradual improvement was observed with prolonged ventilatory support and frequent bronchoscopic monitoring.

By the final bronchoscopy on January 8, 2025, granulation tissue had completely regressed, and the prolonged tracheostomy tube was no longer necessary (Fig. 2). A standard tracheostomy tube was successfully placed, highlighting the effectiveness of conservative airway management in resolving tracheal granulation without invasive intervention.

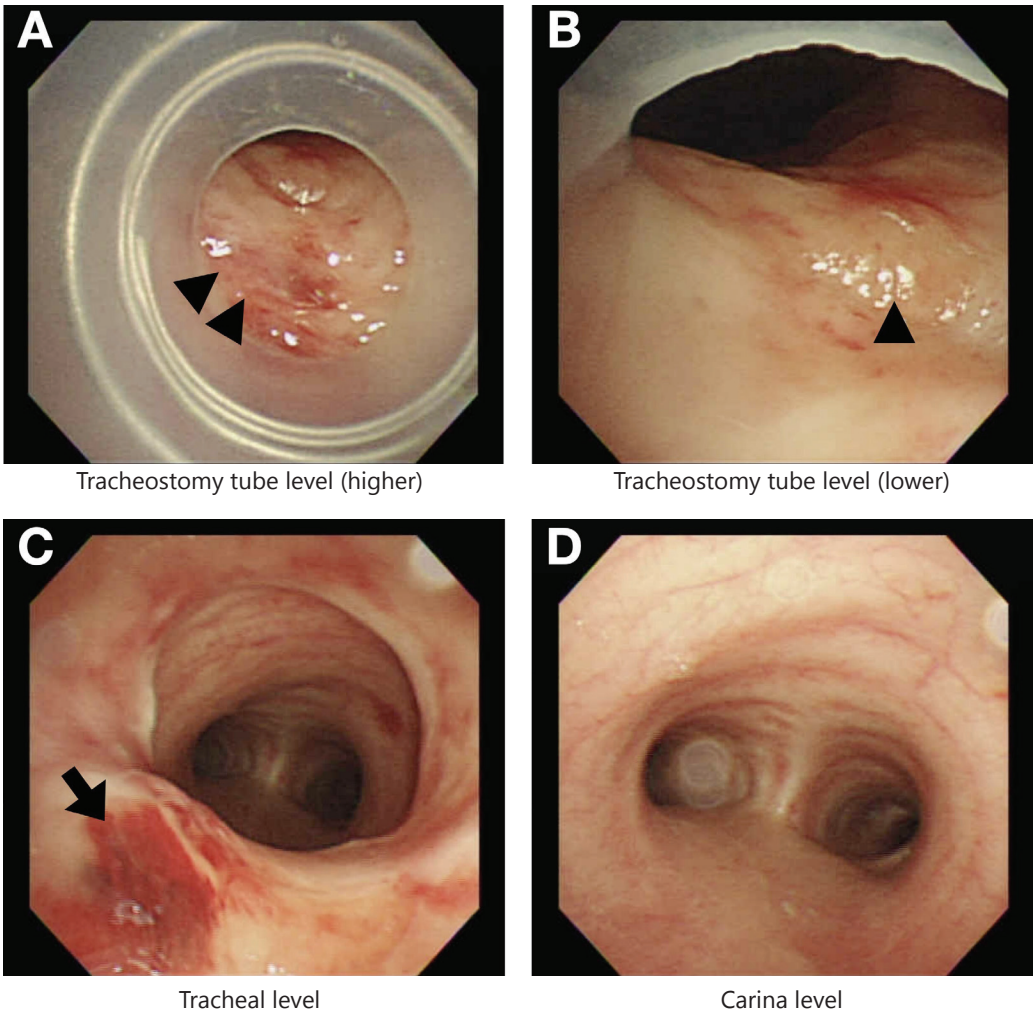

Fig. 1. Bronchoscopy on June 28, 2024, revealed circumferential granulation tissue at the middle-third of the trachea (black triangle, A and B), with mucosal erosion (black arrow, C), causing luminal narrowing at the tracheostomy opening (A and B). The airway remained patent at the carina level (D).

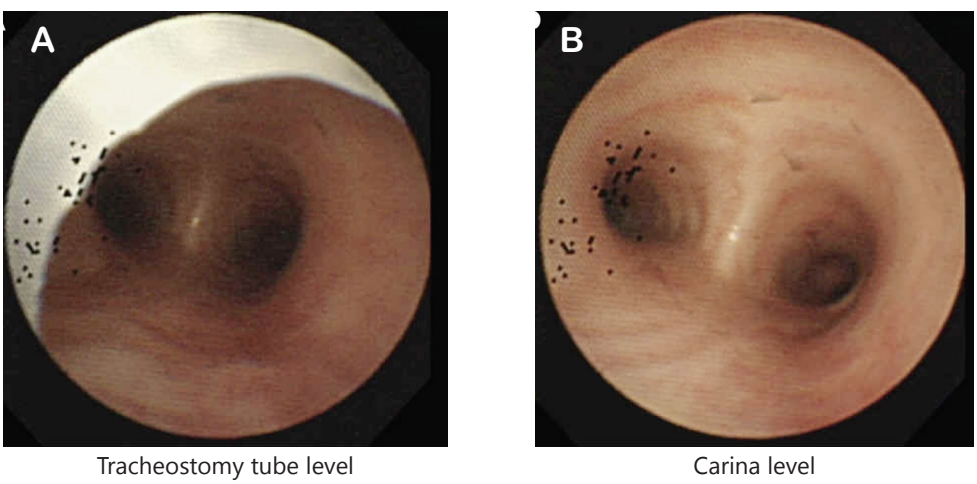

Fig. 2. By the final bronchoscopy on January 8, 2025, granulation tissue had completely regressed over the tracheostomy tube level (A) and carina level (B), and the prolonged tracheostomy tube was no longer necessary.

Discussion

As is well known, tracheal granulation is a common complication in both pediatric and adult tracheostomized patients, often leading to airway obstruction and significant difficulty in weaning from MV [1-2]. Over the past decades, pediatric and thoracic surgeons have explored various strategies to prevent its formation, particularly in children and young adults. In adult patients, a widely recognized preventive measure is the routine exchange of tracheostomy tubes to reduce granulation tissue formation [5]. However, there is no established clinical consensus on the optimal frequency for tube changes in long-term tracheostomized patients. High-functioning individuals typically undergo tube exchanges every 6 months, whereas those with more complex airway issues require more frequent changes, ranging from every 1 to 3 months [6]. In our case, due to the severity of airway complications, tracheostomy tube changes were performed even more frequently, at a monthly interval.

When tracheal granulation tissue is identified, it significantly worsens the prognosis for ventilator weaning and increases the risk of prolonged respiratory failure [1]. Timely and appropriate management is crucial, particularly when airway obstruction occurs. Among the widely used interventions, laser and surgical techniques, including APC, neodymium-doped yttrium aluminum garnet laser, carbon dioxide laser, and holmium-doped yttrium aluminum garnet laser, have demonstrated success in clearing obstructive granulation tissue and restoring airway patency [1, 3, 7]. Pharmacological treatments, such as inhaled budesonide, have also been shown to be effective in reducing postoperative granulation tissue in congenital tracheal stenosis, thereby decreasing the need for additional interventions like balloon dilatation and stenting [8]. Additionally, tranilast, when combined with APC, has proven beneficial in treating airway obstruction caused by granulation tissue following tracheal anastomosis [3].

In more refractory cases, surgical techniques like the stent-in-stent method and the use of adjustable flange tracheostomy tubes have been applied to control excessive granulation tissue hyperplasia while preventing further complications [9]. More recently, drug-eluting coatings on tracheal stents have emerged as a promising approach to minimize granulation tissue formation. Various polymer materials, including polylactic acid (PLA), poly(lactic-co-glycolic acid), and polycaprolactone, have shown effectiveness in reducing tissue overgrowth, with PLA-based coatings showing superior retention of therapeutic agents and inhibition of granulation formation in vivo [10].

Conservative management of tracheal granulation, particularly post-tracheostomy, can be an effective non-surgical approach in selected cases. Studies have reported favorable outcomes, with successful interventions demonstrating the potential for tracheal granulation resolution without invasive procedures [11]. In our case, best supportive care combined with monthly bronchoscopy-guided tracheostomy tube adjustments resulted in near-total resolution of the granulation tissue. However, conservative management should not be universally applied to all patients, as its success depends on various factors, including the size and location of the granulation tissue, the patient's overall health, and underlying conditions. Identifying specific predictive factors for favorable outcomes remains challenging due to the limited

number of cases available for analysis. In our patient, close monitoring and conservative management successfully alleviated tracheal granulation, although this may not directly translate into ventilator liberation or improved long-term respiratory outcomes. Furthermore, whether the resolution of granulation tissue directly correlates with a higher weaning success rate or improved prognosis remains a topic of ongoing debate.

Conclusions

Tracheal granulation poses a significant challenge in tracheostomized patients, often leading to airway obstruction and prolonged ventilator dependence. Although ablative therapies such as laser or APC are commonly used, our case shows that conservative management, including frequent bronchoscopic evaluations and monthly tracheostomy tube adjustments, can successfully resolve granulation tissue. However, patient selection is crucial, as not all cases are suitable for non-invasive approaches. Further research is needed to establish optimal management strategies and assess the impact of granulation resolution on weaning outcomes. Individualized treatment remains key to improving airway patency and respiratory care in tracheostomized patients.

References

1. Heunks LM, van der Hoeven JG. Clinical review: the ABC of weaning failure--a structured approach. Crit Care 2010; 14(6): 245.
2. Cipriano A, Mao ML, Hon HH, *et al*. An overview of complications associated with open and percutaneous tracheostomy procedures. Int J Crit Illn Inj Sci 2015; 5(3): 179-188.
3. Sato M, Terada Y, Nakagawa T, *et al*. Successful use of argon plasma coagulation and tranilast to treat granulation tissue obstructing the airway after tracheal anastomosis. Chest 2000; 118(6): 1829-1831.
4. Madden BP, Datta S, McAnulty G. Tracheal granulation tissue after percutaneous tracheostomy treated with Nd:Yag laser: three cases. J Laryngol Otol 2001; 115(9): 743-744.
5. Yaremchuk K. Regular tracheostomy tube changes to prevent formation of granulation tissue. Laryngoscope 2003; 113(1): 1-10.
6. Spiller P, Dewan K, Kost KM, *et al*. Established adult tracheostomy tube exchange: how often is enough? Laryngoscope 2024; 134(7): 2985-2986.
7. Yang Y, Wang LY, Zhang L, *et al*. Management strategies of granulation in tracheal post-tracheostomy caused by prolonged mechanical ventilation. Lin Chuang Er Bi Yan Hou Tou Jing Wai Ke Za Zhi 2018; 32(11): 857-859.
8. Yokoi A, Nakao M, Bitoh Y, *et al*. Treatment of postoperative tracheal granulation tissue with inhaled budesonide in congenital tracheal stenosis. J Pediatr Surg 2014; 49(2): 293-295; discussion 295.
9. Xie PF, Liu Y, Qi Y, *et al*. Stent-in-stent technique for removal of the tracheal stent in patients with severe granulation tissue hyperplasia. Quant Imaging Med Surg 2021; 11(11): 4676-4682.
10. Sindeeva OA, Prikhozhdenko ES, Schurov I, *et al*. Patterned drug-eluting coatings for tracheal stents based on PLA, PLGA, and PCL for the granulation formation reduction: in vivo studies. Pharmaceutics 2021; 13(9).
11. Gomez-Caro Andres A, Moradiellos Diez FJ, Ausin Herrero P, *et al*. Successful conservative management in iatrogenic tracheobronchial injury. Ann Thorac Surg 2005; 79(6): 1872-1878.

Lung Carcinosarcoma with pre-operative Presentation of Adenocarcinoma and Small cell Carcinoma

Chun-Yen Chen[1], Wei-Ciao Wu[1]

A 53-year-old man suffered from hemoptysis for 2 months. Chest/heart computed tomography (CT) revealed a 9.5x7.3x7.6-cm mass at the left upper lobe (LUL) with air pockets within. Bronchoscopy was performed and the cell block showed many clusters of malignant cells admixed with many macrophages and neutrophils. Adenocarcinoma was favored. CT-guided biopsy was done the next day and pathology showed a small cell malignant tumor. Since the symptoms of hemoptysis persisted, video-assisted thoracoscopic surgery LUL lobectomy was performed without incidence and a specimen was sent for examination. Post-operation pathology showed carcinosarcoma. We also compared pre-operative and postoperative immunohistochemical studies. ***(Thorac Med 2026; 41: 44-47)***

Key words: carcinosarcoma, adenocarcinoma, small cell carcinom

Introduction

Carcinosarcoma is more frequently described in the uterus, esophagus, and skin, and is unusual in the lung. Pathology of carcinosarcoma reveals malignant epithelial and mesenchymal cells. Pulmonary sarcomatoid carcinoma (PSC) has a low incidence (from 0.3% to 3%) among all primary lung malignancies. The median age at diagnosis is about 65 years. Standard therapy for PSC has not yet been established owing to the low incidence of this tumor. Complete surgical resection is the first choice of treatment for PSC.

Case Presentation

A 53-year-old smoking male (1 pack/day for 30 years) presented to a local hospital with the symptom of hemoptysis for 2 months. Chest computed tomography (CT) revealed a 9.5x7.3x7.6-cm mass at the left upper lobe (LUL), with air pockets within (Fig. 2, Fig. 3). Bronchoscopic biopsy revealed many clusters of malignant cells admixed with many macrophages and neutrophils. Adenocarcinoma was

[1]Division of Thoracic Surgery, Division of Surgery, Shuang Ho Hospital, Taipei Medical University, Taipei, Taiwan.
Address reprint requests to: Dr. Wei-Ciao Wu, Division of Thoracic Surgery, Department of Surgery, Shuang Ho Hospital, Taipei Medical University, No.291, Zhongzheng Rd., Zhonghe District, New Taipei City 23561, Taiwan.

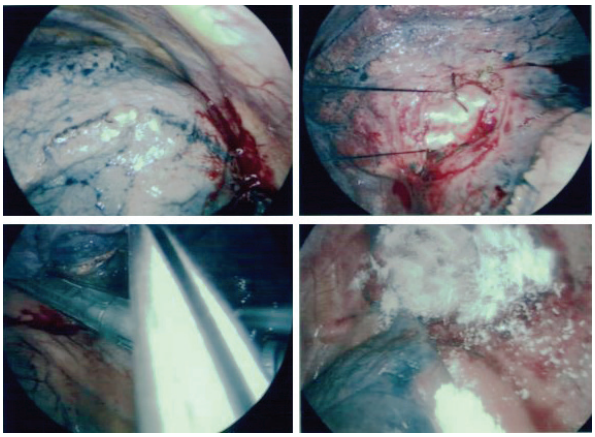

Fig. 1. Photos????, Images???? of the left upper lobe lobectomy and radical lymph node dissection using video-assisted thoracoscopic surgery.

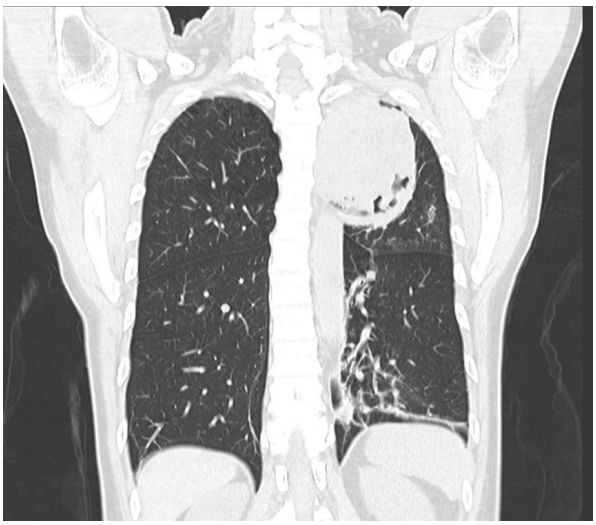

Fig. 2. Chest computed tomography (CT) coronal view revealing a 9.5x7.3x7.6-cm mass at the left upper lobe with air pockets within.

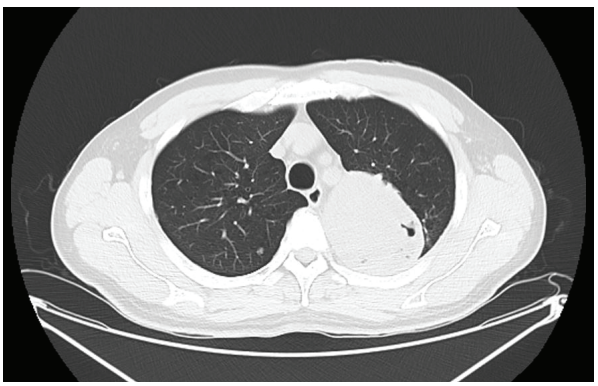

Fig. 3. Chest computed tomography (CT) axial view showing a 9.5x7.3x7.6-cm mass at the left upper lobe with air pockets within.

favored. Percutaneous CT-guided needle biopsy of the lung tumor was performed the next day, and the diagnosis of small cell malignant tumor was made. Since the symptoms of hemoptysis persisted, we performed LUL lobectomy and radical lymph node dissection with video-assisted thoracoscopic surgery (Fig. 1).

Macroscopically, the lesion was a ruptured, necrotic, gray, soft tumor measuring 7.5 x 7.5 x 5.0 cm in size, with a well-defined border, located at central and peripheral regions, 2.0 cm from the bronchial margin.

Immunohistochemical studies showed that the tumor was positive for CK (carcinoma), TTF-1 (carcinoma), claudin-4 (carcinoma), CD56, desmin (focal), myogenin (focal), synaptophysin (focal), INSM1 (very focal), SALL4 (focal), PAX8 (focal), and TLE-1, and was negative for EMA, chromogranin A, ETV4, p40, NKX3.1, NUT, and EBER. H3K27me3 and SMARCA4 showed retained nuclear expression (Fig. 4, Fig. 5), and beta-catenin showed cytoplasmic staining. S100 was negative generally, but positive in the chondrosarcomatous focus (Fig. 6).

Microscopically, the lesion was revealed as a biphasic tumor with a carcinomatous component, i.e., adenocarcinoma, and a sarcomatous component, which included a heterologous chondrosarcomatous focus. The differential diagnoses included carcinosarcoma and pulmonary blastoma. However, due to the lack of nuclear expression of the beta-catenin, a diagnosis of carcinosarcoma was favored.

Discussion

Carcinosarcomas are defined as tumors consisting of an admixture of malignant epithelial and mesenchymal elements. They are more

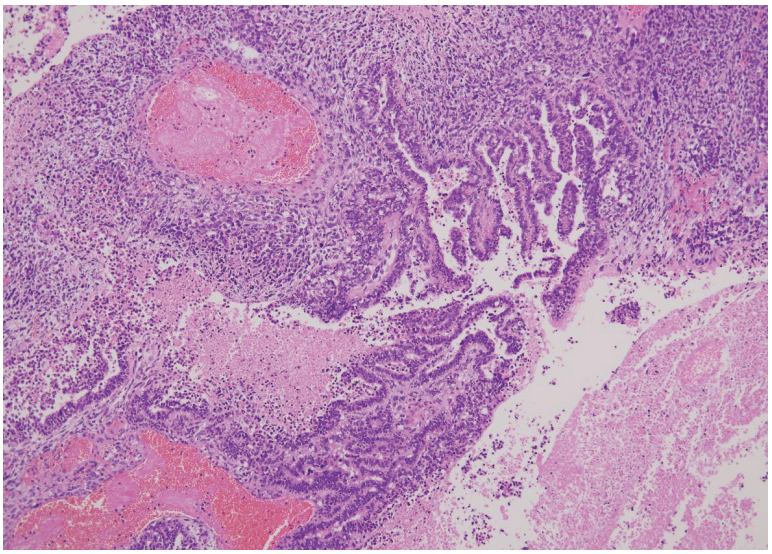

Fig. 4. Histology of the resected specimen with H&E-staining, highly suggestive of moderately to poorly differentiated adenocarcinoma.

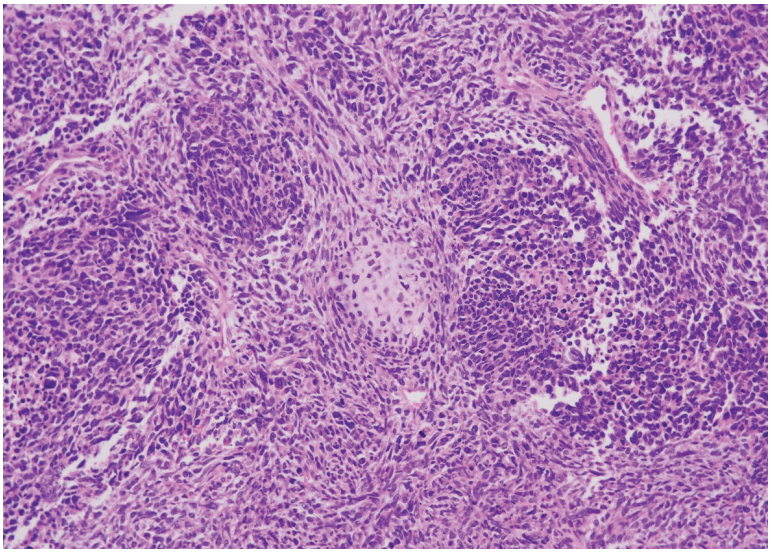

Fig. 5. Histology of the resected specimen with H&E-staining showing nodular aggregation of epithelioid histiocytes.

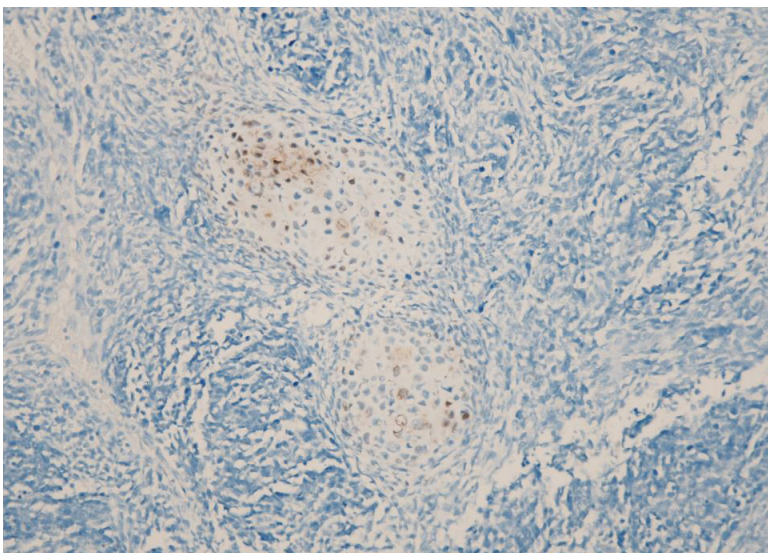

Fig. 6. Carcinosarcoma typically presenting dual positivity—epithelial markers and mesenchymal markers with immunohistochemistry (IHC) staining.

frequently described as present in the uterus, esophagus, skin, lung, and hypopharynx, and are included in a group of poorly differentiated non-small cell lung carcinomas that contain a component of sarcomatoid differentiation, so-called sarcomatoid carcinoma.

In 2004, according to the World Health Organization classification of lung tumors, sarcomatoid carcinomas were classified into 5 subtypes: pleomorphic carcinoma, spindle cell carcinoma, giant cell carcinoma, carcinosarcoma, and pulmonary blastoma [1-2]. PSC is a heterogeneous category of primary lung cancer, accounting for 0.3% to 3% of all primary lung malignancies. In spite of its anaplastic characteristics, many cases of PSC are completely resectable [3-4].

The median age at diagnosis is about 65 years, although pulmonary blastoma usually affects younger smokers without a gender predilection. Standard therapy for PSC has not yet been established owing to the low incidence of this tumor. Complete surgical resection is the first choice for PSC. Metastases are common to the regional lymph node, followed by the brain, bone, kidney and liver. Overall, PSC has a worse prognosis than conventional non-small cell carcinoma due to the greater tendency for distant metastasis, particularly when the sarcomatous component is predominant [5].

Chemotherapeutic agents, such as doxorubicin, adriamycin, ifosfamide and dacarbazine, are known to be effective. If distant metastasis occurs, a combination with chemotherapy is indicated. The overall response rate after systemic treatment of advanced tumors is estimated to be 40% in soft tissue sarcomas [6-7].

In conclusion, we presented a rare case of sarcomatoid carcinoma. PSC is a highly heterogeneous tumor group, and has a poorer prognosis than other epithelial non-small cell lung carcinomas. The results of surgical treatment of PSC are relatively satisfactory, and significant prognostic factors are tumor diameter and stage [8].

References

1. Baldovini C, Rossi G, Ciarrocchi A. Approaches to tumor classification in pulmonary sarcomatoid carcinoma. Lung Cancer (Auckl) 2019 Dec 5; 10: 131-149. doi: 10.2147/LCTT.S186779
2. Devi P, Singh N, Tortora MJ. Pulmonary carcinosarcoma: a case report of biphasic lung tumor. Cureus 2019 Sep 13; 11(9): e5643. doi: 10.7759/cureus.5643
3. Braham E, Ben Rejeb H, Aouadi S, *et al*. Pulmonary carcinosarcoma with heterologous component: report of two cases with literature review. Ann Transl Med 2014; 2(4): 41. doi:10.3978/j.issn.2305-5839.2014.02.10
4. Bull JC Jr, Grimes OF. Pulmonary carcinosarcoma. Chest 1974 Jan; 65(1): 9-12. doi: 10.1378/chest.65.1.9. PMID: 4809344.
5. Pang A, Carbini M, Moreira AL, *et al*. Carcinosarcomas and related cancers: tumors caught in the act of epithelial-mesenchymal transition. J Clin Oncol 2018 Jan 10; 36(2): 210-216. doi: 10.1200/JCO.2017.74.9523. Epub 2017 Dec 8. PMID: 29220296.
6. Olobatoke AO, David D, Hafeez W, *et al*. Pulmonary carcinosarcoma initially presenting as invasive aspergillosis: a case report of previously unreported combination. Diagn Pathol 2010 Jan 29; 5:11. doi: 10.1186/1746-1596-5-11. PMID: 20181054; PMCID: PMC2851579.
7. Zhang Z, Chen Y, Ma M, *et al*. Significant benefit of Nivolumab treating PD-L1 positive metastatic pulmonary carcinosarcoma: a case report and literature review. Oncotarget 2017 Jul 7; 8(56): 96453-96459. doi: 10.18632/oncotarget.19089. PMID: 29221220; PMCID: PMC5707114.
8. Sayan M, Bas A, Valiyev E, *et al*. Prognostic factors for sarcomatoid carcinomas of lung: a single-centre experience. Lung India 2020; 37(6): 506-510. doi:10.4103/lungindia.lungindia_525_19.